

Spring 4-13-2019

MACHINE LEARNING APPLICATIONS IN COMPUTER INTEGRATED MATERIAL DESIGN AND MODELING

Joseph O. Oyedele
University of Texas at Tyler

Follow this and additional works at: https://scholarworks.uttyler.edu/me_grad

 Part of the [Materials Science and Engineering Commons](#)

Recommended Citation

Oyedele, Joseph O., "MACHINE LEARNING APPLICATIONS IN COMPUTER INTEGRATED MATERIAL DESIGN AND MODELING" (2019). *Mechanical Engineering Theses*. Paper 5.
<http://hdl.handle.net/10950/1334>

This Thesis is brought to you for free and open access by the Mechanical Engineering at Scholar Works at UT Tyler. It has been accepted for inclusion in Mechanical Engineering Theses by an authorized administrator of Scholar Works at UT Tyler. For more information, please contact tbianchi@uttyler.edu.

MACHINE LEARNING APPLICATIONS IN COMPUTER INTEGRATED
MATERIAL DESIGN AND MODELING

by

JOSEPH O. OYEDELE

A thesis submitted in partial fulfillment
of the requirements of the degree of
Master of Science in Mechanical Engineering
Department of Mechanical Engineering

Chung Hyun Goh, Ph. D., Committee Chair

College of Engineering

The University of Texas at Tyler
May 2019

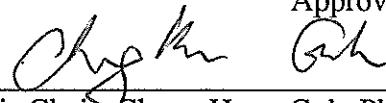
The University of Texas at Tyler
Tyler, Texas

This is to certify that the Master's Thesis of

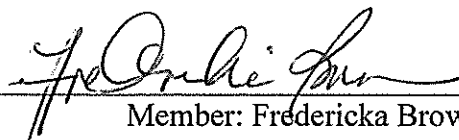
JOSEPH O. OYEDELE

has been approved for the thesis requirement on
April 15, 2019
for the Master of Mechanical Engineering degree

Approvals:



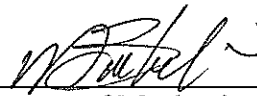
Thesis Chair: Chung Hyun Goh, Ph.D.



Member: Fredericka Brown, Ph.D.



Member: Shih-Feng Chou, Ph.D.



Chair, Department of Mechanical Engineering



Dean, College of Engineering

© Copyright by JOSEPH O. OYEDELE 2019
All rights reserved

Acknowledgments

All praise is to the Al-Mighty God, for the grace and protection throughout the entire time until the completion of this thesis.

I would like to express my gratitude and appreciation to my thesis advisor, Dr. Chung Hyun Goh, for his constant guidance and continuous support throughout this research process. His knowledge and profound expertise helped me through this thesis.

I would also like to thank my thesis committee members, Dr. Fredericka Brown and Dr. Shih-Feng Chou for their kind support and willingness to assist with my thesis. I want to express my gratitude to Dr. Muthukrishnan Sathyamoorthy and Dr. Chung Hyun Goh for giving me the opportunity to work as a Teaching Assistant in the department. I would like to thank all staff members, colleagues, and friends in the Mechanical Engineering Department for their kind support. Finally, I'm extremely pleased to have received enormous support from my family and want to express my sincere appreciation and gratitude to them. In particular I would like to thank my brother Adewale, who supported me and helped me financially throughout my studies, Toyin and David for their moral support, and finally, my Mom and Dad for their constant encouragement and prayers. My appreciation also goes out to my colleagues and friends, Alireza, Armin, Anika, and Kirill, for their technical assistance and encouragement as well. I will always remember the assistance, kindness, and cooperation from all those mentioned above.

Table of Content

List of Tables	iii
List of Figures	iv
Abbreviations	vi
Nomenclature	vii
Abstract	viii
Chapter 1. Introduction	1
1.1 Overview	1
1.2 Research Objective	5
1.3 Research Question	5
1.4 Working Hypothesis	5
1.5 Tasks	5
1.6 Machine Learning	5
1.7 Organization of Thesis	8
Chapter 2. The Inverse Hierarchical Analysis	9
2.1 Introduction	9
2.2 Literature Review.....	9
2.3 Design Approach	12
2.4 Results and Discussion	20
2.5 Closure and future work.....	23
Chapter 3. A Predictive Machine Learning Approach to Time Temperature Transformation Diagram Modeling in Material Design	25
3.1 Introduction	25
3.2 Literature Review	25
3.3 Design Approach	26
3.4 Results and Discussion	30
3.5 Closure and future work	34

Chapter 4. AI Adoption to Modeling Constitutive Behavior	35
4.1 Introduction	35
4.2 Literature review	35
4.3 Design Approach	38
4.4 Results and Discussion	42
4.5 Closure and future work	42
Chapter 5. Validation using Finite Element Method (ANSYS)	43
5.1 Inverse Hierarchical Analysis Model for the Hot Rolling Process	43
5.2 Constitutive Model Prediction of a Flexinol Wire	47
Chapter 6. Closure and Future work	50
References	52
Appendices	57
Appendix A: Monte Carlo Algorithm	57
Appendix B: Random Forest Algorithm	58
Appendix C: ANSYS Report File and Tables	60

List of Tables

Table 1. Dependent parameters for IHA.....	19
Table 2. Independent parameters for IHA	19
Table 3. Feasible ranged solution set for the forward modeling	23
Table 4. Feasible ranged solution set for the inverse modeling	23
Table 5. Chemical composition of A8 Steel	29
Table 6. Properties of flexinol wire	39
Table 7. Performance variable evaluation by FE Analysis	46
Table 8. IHA predicted values across P-S-P-P structure	46
Table 9. Elastic behavior of different constitutive behavior model	49
Table 10. Plastic behavior of different constitutive behavior model.....	49

List of Figures

Figure 1. Sequential schematic diagram of the integrated design of materials and products	2
Figure 2. An example of information flow in a model chain.....	2
Figure 3. Conceptual framework of the IHA for the P-S-P-P linkage.....	4
Figure 4. Process flow for modeling the TTT curve and constitutive behavior of steel.....	4
Figure 5. Process flow of a new material design.....	6
Figure 6. A sequential exploration process for integrated design in the IHA	11
Figure 7. A schematic of the regression model	14
Figure 8. Feasible regions indicating desirable design spaces in Structure spaces	21
Figure 9. Feasible regions indicating property space and performance space	22
Figure 10. Monte Carlo algorithm.....	28
Figure 11. Random data sample generated with Monte Carlo simulation.....	30
Figure 12. Upper bound plot with Monte Carlo method	31
Figure 13. Lower bound plot with Monte Carlo method	31
Figure 14. Super-position of the upper and lower bound plot	32
Figure 15. Plot of time temperature transformation diagram with random forest model..	33
Figure 16. Typical microstructure of steel with perlitic grain structure and eutectoid composition	35
Figure 17. Set data for the set experiment with 75°C temperature applied to the flexinol wire	39
Figure 18. Constitutive behavior plot for flexinol wire at 75°C using the intercept method	40
Figure 19. Constitutive behavior plot for flexinol wire at 75°C after applying Monte Carlo method	41
Figure 20. Constitutive behavior plot for Flexinol wire at 75°C consisting of the RF prediction and the Monte Carlo generated data set	41

Figure 21. A roll pass design.....	43
Figure 22. 3D Model of a hot rolling simulation process	44
Figure 23. Surface bodies of the 3D hot rolling process.....	45
Figure 24. Factor of safety simulation result	46
Figure 25. 3D constitutive model for flexinol with boundary conditions	47
Figure 26. Stress-strain curve of a material modeled after flexinol material properties...	48

Abbreviation

AGS	Austenite Grain Size
ATC	Analytical Target Cascading
AI	Artificial Intelligence
ANN	Artificial Neural Network
ANOVA	Analysis of Variance
BCC	Body Centered Cubic
BNC	Bayesian Network Classifier
CCT	Continuous Cooling Transformation
CR	Cooling Rate
FCC	Face Centered Cubic
FS	Factor of Safety
FGS	Ferrite Grain Size
FEA	Finite Element Analysis
IDEM	Inductive Design Exploration Method
IHA	Inductive Hierarchical Analysis
ML	Machine Learning
PDF	Probability Distributed Function
P-S-P-P	Process-Structure-Property-Performance
RF	Random Forest
RMSE	Root Mean Square Error
SMAs	Shape Memory Alloys
SVDD	Support Vector Domain Description
TTT	Time Temperature Transformation

Nomenclature

k	Smoothing Parameter
M	Number of trees in the forest
$m_{M,n}$	Regression Error Estimate
\mathbb{N}	Set of Natural Numbers
T	Temperature
T_n	Training Samples
Y	Predicted (output) Variable
$\alpha_1, \alpha_2, \dots, \alpha_n$	Set of factors
$\Theta_1, \dots, \Theta_M, \psi, X$	Independent Variables
β	Sample of n Observations

Abstract

MACHINE LEARNING APPLICATIONS IN COMPUTER INTEGRATED MATERIAL DESIGN AND MODELING

Joseph O. Oyedele

Thesis Chair: Chung Hyun Goh, Ph.D.

The University of Texas at Tyler
May 2019

This research seeks to develop and test a framework for considering Inductive Hierarchical Analysis (IHA) using Machine Learning (ML) technique in a multistage material design of a gear manufacturing process. A ML model was developed, which implements Random Forest (RF) regression algorithm together with analysis of variance (ANOVA) approach for mapping sets of material and product design variables, thus classifying the design space into feasible and non-feasible solution space. This approach is applied to the design of steel gear within specified performance requirements by exploring the design space for the Process-Structure-Property-Performance (PSPP) relation in the hot rolling process. With an objective of how machine learning models can be incorporated into the material design and modeling for predicting the material properties of steel used for gear manufacturing, a working hypothesis was outlined, and tasks for accomplishing this objective was developed. Feasible solution space was derived by the RF approach across the PSPP chain for the gear design by considering forward and inverse mapping. For the forward process, feasible range set of 84.68 - 84.9 and 32.54 - 32.84 was mapped at the structural stage to give feasibility range of 193.169 - 193.1818 at the property stage and eventually a feasibility range of 1.578 - 1.676 for the performance stage. The feasibility range was used as an input for the inductive process to generate feasible region of 193.171 - 193.174 at the property stage, 32.61 - 32.69 and 84.41 - 84.70 at the structural

stage, while a feasible range of 1340 - 1360K evolved at the processing stage. The inverse process shows propagated reduction in variable size across the PSPP linkage with a Root Mean Square Error value of 6.665×10^{-5} . This indicates a negligible error propagation across the modeling analysis and shows the robustness of RF as an ensemble of multiple decision trees. To further test the developed model, a predictive analysis of the Time-Temperature Transformation (TTT) curve was carried out by implementing Monte Carlo simulations together with the RF algorithm. This method accurately predicts the TTT curve with an accuracy matrix of 92.7%. The application of Monte Carlo helps to increase the robustness of the RF model by generating more input data points.

This research work was extended to model the constitutive behavior of a flexinol wire to incorporate Artificial Intelligence (AI) with Finite Element Methods (FEM) as a way validating the approaching methods in this research. Being able to implement machine learning applications to computer integrated material design and modeling presents a novel approach to material design by using RF method. This broadens the knowledge base in material design processing and opens up opportunities for further research with the application of RF to material design. In addition, this research will help in bridging the gap and timeline in meeting customer's performance requirements by serving as a tool for designing materials that are feasible with optimum performance capability for any engineering need.

Chapter 1

Introduction

1.1 Overview

Over time, engineering materials and product design paradigms follow the conventional way of selecting materials from databases of materials and their properties. The traditional way of designing engineering materials typically involves considering material properties at the macro level. However, the exact and suitable material properties that are needed for most technical requirements are often not feasible or simply do not satisfy the design needs. This consequently limits the performance capabilities of many systems and available products and, thus, creates the need for improved system performance. But in recent years, a more advanced wave of material design has emerged, and it involves fabricating materials at the nanoscale. This has led to the concurrent design of material microstructure and composition alongside system level design. This new paradigm in engineering is enabling scientists and engineers to design a new class of materials that meet product and performance requirements.

Most of the multidisciplinary design optimization methods such as Analytical Target Cascading (ATC), concurrent subspace optimization, etc. require an expensive iterative simulation analysis among design levels. To eliminate these challenges, researchers have developed methods to optimize design methods. Chen et al. applied ATC with metamodels to solve multiscale design problems [1]. This, however, yielded little improvement as metamodels perform poorly on discrete variables and discontinuous output responses that often characterize material design problems. The multilevel design method for steel and other materials is comprised of sequential deductive analyses represented by a bottom-up mapping. This involves the transitioning from processing level to the microstructure stage, to the material properties stage, and then finally to the performance stage. Inversely, inductive (top-down) sequential analysis achieves the design goal by following the stages in reverse order, as shown in Fig 1.

The set-based approach to solving the design problem, however, provides a decoupling analysis approach to multilevel design problems in a decentralized manner, thus reducing number of iterations and providing range-sets of feasible solution points across different levels of the multiscale design problem.

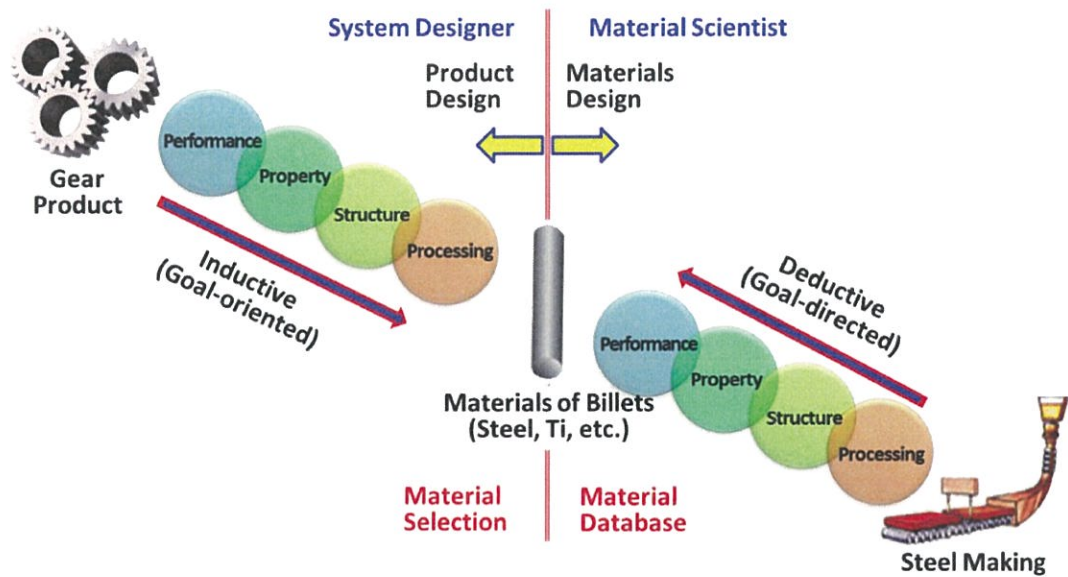


Figure 1. A schematic sequential diagram of the integrated design of materials and products [2]

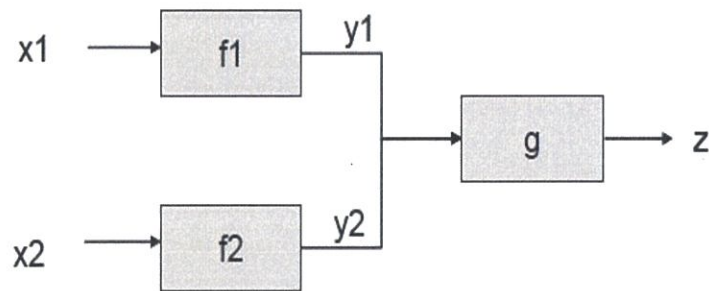


Figure 2. An example of information flow in a model chain [3]

The information flow for a simple multi-stage model case is shown in Fig. 2 [2]. Here x_1 and x_2 represent the input design variables or parameters related to the process level. Functions f_1 and f_2 predict the simulation material properties y_1 and y_2 . The material properties y_1 and y_2 are seen as output parameters for the processing functions f_1 and f_2 , respectively. These material properties become input parameters for the mapping function g to predict a system level response z . This case scenario for a multistage analysis shows an interdependence of models from the input design stages x_1 and x_2 to the system requirement stage z . Uncertainty may be accumulated and propagated through

the sequence if unchecked, leading to an amplified propagated uncertainty in the final system response. Several modeling approaches have been employed to reduce and possibly eliminate the propagation of uncertainty in multi-stage modeling. Taguchi proposed a robust design in the process of reducing the effect of uncertainties [3]. This design robustness makes the system insensitive to uncertainties. To reduce or eliminate uncertainty propagation in a model, the type of the accumulated or propagated uncertainty needs to be determined [4].

Uncertainties have been classified based on several evaluations. Effective analysis of these uncertainties is key to a successfully robust design process. A broad category of uncertainty analysis is the probabilistic and non-probabilistic method based on the type of uncertainty. The probabilistic approach is further categorized as statistical and non-statistical. Monte Carlo simulation are classified under the statistical method. However, the available uncertainty evaluation methods have some shortcomings, such as large computation time and high cost of experiment analysis. A robust design process was proposed to be insensitive to uncertainties without eliminating them. These designs consist of the Type I, Type II, Type III, and Type IV robust designs in sequential order. The Type II robust design is an improvement of the Type I design. Also, the Type IV robust design is an improvement of the Type III design process. The improvement in these robust designs up to the Type IV design model suggests that each of the previous models have shortfalls that make them non-feasible for uncertainty analysis. The Type IV design employs the Inductive Design Exploration Method (IDEM) in robust design to reduce the effect of uncertainties in system design. This process is done by finding the feasible solution range of a data set through inductive hierarchical exploration of the design space and through parallelization of multiple function evaluations [1][4][5]. This method discretizes an N dimensional space of independent variables into an N dimensional space of discrete possible solutions. Each possible solution is evaluated by considering the Hyper Dimension Error Margin Index (IDEM) to determine feasible solution sets. IDEM has its shortcomings, as it is very computationally expensive because it requires an exhaustive search of possible solutions at each level of the multistage design. To address the varying challenges to providing solutions to the multilevel design problem, various ML approaches have been utilized.

In Fig. 3, the performance parameters from the deductive analysis become the input data for the RF model as shown. RF algorithm in R was implemented with ANOVA to perform regression analysis and predict the process parameters. FEA modeling in ANSYS was incorporated as a validation method for the hot rolling process.

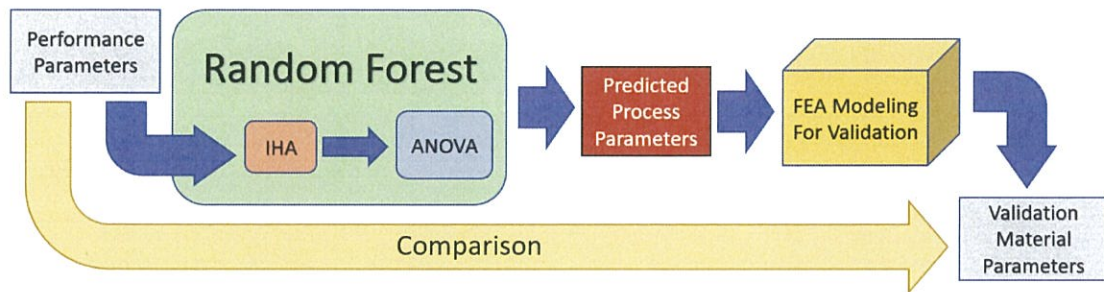


Figure 3. Conceptual framework of the IHA for the PSPP linkage

In Fig. 4, dataset samples for both the TTT curve of A8 steel and the constitutive behavior of flexinol wire were extracted. These dataset samples then imported as the input data for the RF model to perform the supervised regression analysis with Monte Carlo simulation. The ML approach resulted in the prediction of a TTT diagram and the constitutive behavior of flexinol wire. FEA modeling was applied as a validation method for the constitutive behavior prediction of flexinol wire. The TTT diagram was validated by comparing predicted results with experimental results.

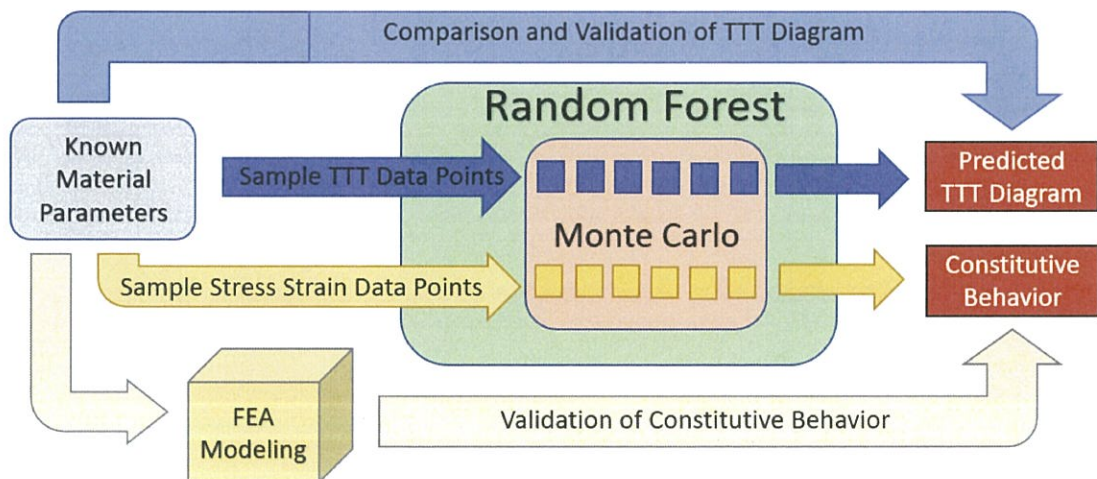


Figure 4. Process flow for modeling the TTT curve and constitutive behavior of steel

1.2 Research Objective

The research objective is to characterize how machine learning models can be incorporated into the material design and modeling for predicting the material properties of steel used for gear manufacturing.

1.3 Research Question

How can we effectively implement a RF model to classify feasible and infeasible regions in the forward and inverse hierarchical analysis across the Process-Structure-Property-Performance (P-S-P-P) stage of the multistage design process?

1.4 Working Hypothesis

With the integration of the Random Forest regression model and ANOVA method in R statistical environment, we can computationally predict feasible and infeasible data points across the P-S-P-P linkage in an inverse hierarchical manner for the gear manufacturing process.

1.5 Tasks

A total of five tasks will be used to address the research question with the working hypothesis:

- Task 1: Develop a RF model implemented with ANOVA and IHA across the P-S-P-P linkage
- Task 2: Conduct performance evaluation and sensitivity analysis of the RF model
- Task 3: Apply the RF model with Monte Carlo simulation to model the TTT curves
- Task 4: Apply the RF model with Monte Carlo simulation to model constitutive behavior of flexinol wire
- Task 5: Verify and validate the RF model using finite element analysis

1.6 Machine Learning

A machine learning (ML) approach to material modeling has been implemented due to the advantages it presents to multi-scale design approach for material and product development. ML is a method of data analysis that automates analytical models. It is the

science of getting computers to learn and act like humans by improving their learning autonomously. This can be done by feeding ML networks with data and information in the form of observations and real-world interactions. Repetitive theoretical characterization and experimental studies are very time consuming and, in most cases, inefficient because significant progress tends to require a combination of chemical intuition and serendipity [6].

It takes up to 20 years for a new material to advance from the initial research stage to its first use. Fig. 5 shows the new material research and its various stages: discovery, development, property, optimization, system design and integration, certification, manufacturing, and deployment. These stages are conducted by different teams and involve few opportunities for feedback across design stages, which could accelerate the discovery process as a whole.

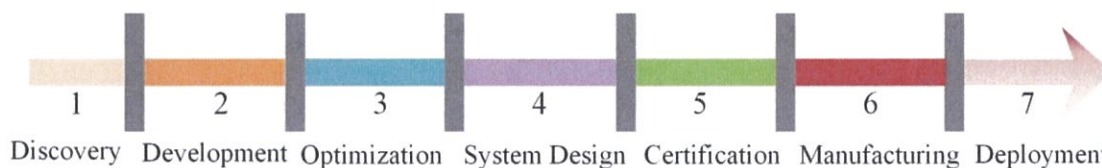


Figure 5. Process flow of a New Material Design [6]

Computational simulations and experimental measurements are two conventional methods that are widely adopted in the field of material science to accelerate material design. However, due to inherent limitations of experimental conditions and theoretical foundations associated with these methods, they are difficult to use. For example, experimental measurements that usually comprise of microstructure and property analysis, measurement, etc. are easy and intuitive ways of materials research even though it must be conducted in an efficient manner over a long period of time.

In addition, this approach demands high requirements ranging from the expertise of the researcher to the experimental environment for the research.

Alternatively to the traditional method used in material design and modeling, computational simulation, ranging from Monte Carlo techniques [7], electronic structure calculations based on density functional theory [8][9], molecular dynamics [10][11], and

the phase-field method [12][13][14] to continuum macroscopic approaches, is another approach in which existing theory is exploited for analysis.

Material design aided by computational simulation has resulted to the discovery of new materials and reduction in materials development time and cost [15]. Computational simulation requires less time in comparison with experimental measurement and is advantageous for supplying real experiments such that one has full control over the relevant variables. Nevertheless, there are several challenges associated with computational simulation. For example, it is strongly dependent on the microstructures of the materials involved; it requires high-performance computing equipment, usually in large computing clusters on which the computational simulation programs can run. Additionally, no explicit use can be made of previous calculation results when a new system is studied. Modern material research often requires close integration of computation and experiment to achieve a fundamental understanding of the structures and properties of the materials of interest and how they are related to the synthesis and processing procedures. In particular, some experiments can be performed virtually using powerful and accurate computational tools, and, thus, the corresponding time frame can be decreased from 10 or 20 years to 18 months or less as required by traditional methods [16][17].

Given the technicality involved in understanding the basic physio-chemical properties of materials and accelerating their applications, both experimental measurements and computational simulations are often incapable of addressing newly emerging issues. For instance, it is very complicated and inefficient to investigate the transition temperature of glass through experimental measurements because the transition occurs over a wide temperature range [18]. However, the glass transition temperature also cannot be exactly simulated using computer programs because it depends on a variety of internal and external conditions such as pressure, structure, and constitutive and conformational features [19]. Therefore, numerous attempts have been made in the field of materials science to develop ways to overcome the shortcomings of these two common methods.

With the launch of the Materials Genome Initiative (MGI) in 2011 and the evolution of the big data era, tremendous progress has been made in the field of materials science to collect extensive datasets of materials properties to provide materials scientists

and engineers with ready access to the properties of known materials, such as the Materials Commons [20], the Open Quantum Materials Database [21], Inorganic Crystal Structure Database [22], the Cambridge Structural Databases [23], the Harvard Clean Energy Project[24], the Materials Project [25], the Materials Data Facility [26], and the superconducting critical temperatures.

A generic data management and sharing platform serves to provide an infrastructure for compelling impetus to accelerate materials discovery and design. Advanced materials characterization techniques, with their growing data acquisition rate and storage capabilities, present a challenge in modern materials science. This creates the need of new procedures for quickly assessing and analyzing collected data [27].

ML is being employed as a powerful tool for finding patterns in high-dimensional data. It employs algorithms through which a computer can learn from empirical data by modeling the linear or nonlinear relationships between the properties of materials and other related factors [28]. In recent times, ML techniques and big data methods have successfully fixed the difficulties of modeling the relationships between materials properties and complex physical factors [29][30].

1.7 Organization of Thesis

This thesis is divided into six chapters. Chapter 1 is an introduction to materials design, modeling, and provides a brief overview on the trend and methods utilized in material design in recent years. Chapter 2 presents an IHA in materials design of mechanical gear along the P-S-P-P structure. Chapter 3 provides information about the modeling of the Time Temperature Transformation (TTT) curve with the approaching methods together with Monte Carlo simulation. Chapter 4 explains the modeling of constitutive behavior of flexinol wire by adopting AI techniques. Chapter 5 explains validation methods of approaching method. Finally, conclusion/closure and future work ideas are presented in Chapter 6.

Chapter 2

The Inverse Hierarchical Analysis

2.1 Introduction

This thesis seeks to develop and test a framework for considering IHA by using a ML approach (RF method) in a multistage material design of the gear manufacturing process. Monte Carlo simulation was further implemented in the predictive modeling of a TTT curve.

The vacuum created by the conventional search method of developing a product by selecting materials based on its properties from existing databases has necessitated recent development in material and product search methodologies. The conventional search method cannot meet up with these demands. It is widely known that within a selected alloy system, the variation in microstructure results in a large range of material properties.

There is a shift in material design in present dispensation where material design and modeling are microstructurally sensitive, and it is crucial to identify the very microstructure within an allowed system out of a system of large candidates that ensured desired property for the product function. Mathematical search-based approach to material design explores the hypothetically, infinitely-large space and presents the freedom of unknown microstructure. With the rapid growth rate of candidate space where microstructure can be represented by thousands of dimensions, the mathematical approach deteriorates.

2.2 Literature Review

ML has proven to be very efficient in material and product design. Researchers have employed several machine learning methods to model material design, and this includes but isn't limited to Artificial Neural Network (ANN), Support Vector Machine, Bayesian Network, and so on. These set-based approaches provide a satisfactory system-wide solution to complex engineering design problems and meet the increased demand for a specific product function. R. Arroyave et al., 2016 implemented Support Vector Domain Description (SVDD) as an approximation to the infinite solution set to determine the feasibility range of a data set while considering some set of thermodynamic conditions for

a phase stability problem [31]. SVDD as a ML technique is a one-class classifier that was used to generate an approximate solution from discrete set points by finding the hypersphere of minimum radius that contains a set N data points. Data points that lie on the hypersphere boundary are the support vectors used to determine the feasible domain description. Jordan Matthews and co-authors applied the Naïve Bayesian Network classifier (BNC), which is a fully disconnected Bayesian network in which no edges existed between design variables to provide mappings between multiscale levels (micro-meso model, and meso-macro model) in the design of Negative Stiffness Metamaterials [32]. The forward modelling generated discrete point sets which are used in back propagation (top to down analysis). BNCs classify sets of training points into high performance points and low performance points by centering the Gaussian probability distributions of these points, (high performance design points and the low performance points) traversing the macro to micro scale through meso scale in an inductive manner. The distribution aggregate forms a Kernel Density Estimate for these points and forms a design boundary generated by points with equal kernel densities. For each scale across the multilevel modeling, specified threshold provides a criterion for finding feasible points at each level. ML predictive modeling was used to predict the microstructure of a machined titanium alloy [35]. Experimental results were used as an input data set for the predictive modelling of micro hardness and grain size. Sixteen samples were generated by varying cutting conditions and then machined. Hardness and microstructure analysis of grain size evolution and volume fraction was conducted by using Scanning Electron Microscope imaging together with a proprietary image processing program written in MATLAB. The temperature field was simulated by using 3D finite element simulations of machining the alloy. This temperature set serves as input dataset to predict hardness using the ML.

In IHA, feasible range sets of material and product specifications are found hierarchically in an inductive manner (i.e., top-down approach). The design of material and product concurrently requires the identification of feasible range sets of data among interconnecting variable functions. From the performance stage and FS range set of data is determined. These data ranges are mapped to the next property stage (UTS) through a variable function. At this point, a feasibility check is carried out on the variable function.

Once this is achieved through the evaluation of ANOVA, the data is passed to the subsequent model stage (FGS, AGS). This process is continued until the feasible range data set for the input variable of the first model are found. This method offers the advantages of analyzing each model stage in a sequential manner as shown in Fig. 6. This results in parallel computation analysis of the whole process, making it easy to update each module in the P-S-P-P linkage.

The IHA was applied to the steel automobile gear manufacturing process to analyze and evaluate product requirement (safety factor) based on design variables at the processing stage (temperature (TK), cooling rate (CR), processing time (t), and billet height (h_i)). This process is done by finding the feasible solution space that satisfy the design variables.

The IHA provides a method that mitigates the propagation of uncertainties in the sequential chain with the use of a large range of dataset and the ANOVA function which check for feasible material function and model function range in an R statistical programming environment at each stage of the P-S-P-P linkage.

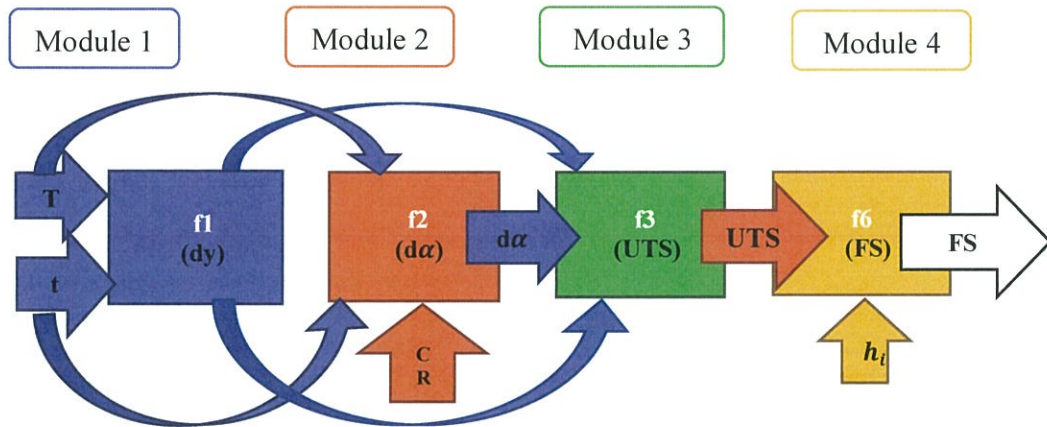


Figure 6. A sequential exploration process for integrated design in the IHA

RF algorithm was implemented together with MATLAB simulations to propagate the hierarchical process. This approach is appropriate for a large, multi-scale material modeling and analysis, as it offers a robust classification of the feasible solution spaces in a timely manner and eliminates noise across the hierarchical process by randomly utilizing

a set of predictors for splitting with a very high prediction accuracy and low variance across variables. This approach uses RF method to successfully map the P-S-P-P spaces in the forward analysis. RF method also conducts inverse propagation or modelling to characterize feasible and infeasible solution spaces across the material/product design.

The robust nature of the process helps in mitigating propagated uncertainties, which tend to arise from the hierarchical inter-model dependence in the multiscale model chain and uncertainty from the material models due to idealization or simplification of models [33].

2.3 Design Approach

ML refers to the automated detection of meaningful patterns in data [33]. It is the application of AI that enables systems to learn and substantiate future decisions from experience without being explicitly programmed. ML algorithms can be divided into three broad categories: supervised learning, unsupervised learning, and reinforcement learning. Supervised learning is useful in cases in which a property (*label*) is available for a certain dataset (*training set*) but is missing and needs to be predicted for other instances. That is, the computer is presented with a range-set of input and output data. The objective of supervised learning is to learn the rule that maps input space to an output space. Unsupervised learning is useful in cases in which the challenge is to discover implicit relationships in a given *unlabeled dataset* (items are not pre-assigned). Reinforcement learning falls between these two extremes. There is some form of feedback available for each predictive step or action, however, there is a lack of precise label or error message.

Supervised learning is categorized based on the expected output of the algorithm. These are primarily in two categories: classification and regression model. In classification model, new predictions are identified to a set of categories that are subset of the same class. Classification model is considered on the instances of supervised learning. When the focus of simulation is on the relationship between dependent variable and sets of independent variables or predictors, a regression model is used. This analysis presents the response of a dependent variable when there is a change in any one of the independent variables while other variables are held constant.

There are several ML algorithms used to carry out training and testing of data set for a required output. The RF method, classified under supervised learning as proposed by Biau, is made up of nearest neighbors whereas “Ni–Mn” indicates an alloy of some composition Ni_xMn_{1-x} algorithm [34]. It is an ensemble of trees that easily captures nonlinear relationships between an input dataset and a target set by using ensemble of regression trees. This predictive model is composed of a weighted combination of multiple regression trees. These models are useful in several prediction tasks where the features are more or less self-evident. In general, the model combines multiple regression trees to increase predictive performance.

The problem structure for our analysis consists of continuous variables that are more than two with several observations. A regression analysis was suitable for this problem because of the continuous nature of the design problem. ANOVA method implementation into RF is the metrics on which feasibility check was performed. ANOVA, known as ANOVA method, is a statistical methodology that determines the variation data points from the mean response of the desired variable. Mathematically, ANOVA is used to analyze the importance of one or more factors by comparing the mean of the response variable at various factor levels. ANOVA requires a continuous response variable and at least a categorical factor with two or more levels. ANOVA require data from approximately normally distributed populations with equal variances between factor levels.

However, ANOVA procedures work quite well even if the normality assumption has been violated, unless one or more of the distributions are highly skewed or if the variances are quite different. Transformations of the original dataset may correct these violations. ANOVA was applied to RF algorithm to determine at what point the individual tree splits to classify each variable into feasible points or infeasible points. Figure 5 shows a general regression tree structure for the analysis considered. The target variable is the dependent variable. Each branch of the tree is created at the point at which the decision is made according to the splitting criteria at each branch node. The response variable for this analysis is continuous and does not belong to any class, thus a regression model is fit to each of the independent variables by isolating these variables as nodes to decrease error. The root node in Fig. 7 depicts the total sample population, or the total data set for the

analysis. The learning process begins at the root node. Internal nodes are formed as the root node splits as decision criteria is met. Recursive partitioning is used to create each internal node. Each internal node contains sets of data that meet the splitting criteria. The splitting process continues till it gets to the leaf or terminal nodes. At this point, all decision criteria are met and further splitting of data set is not possible.

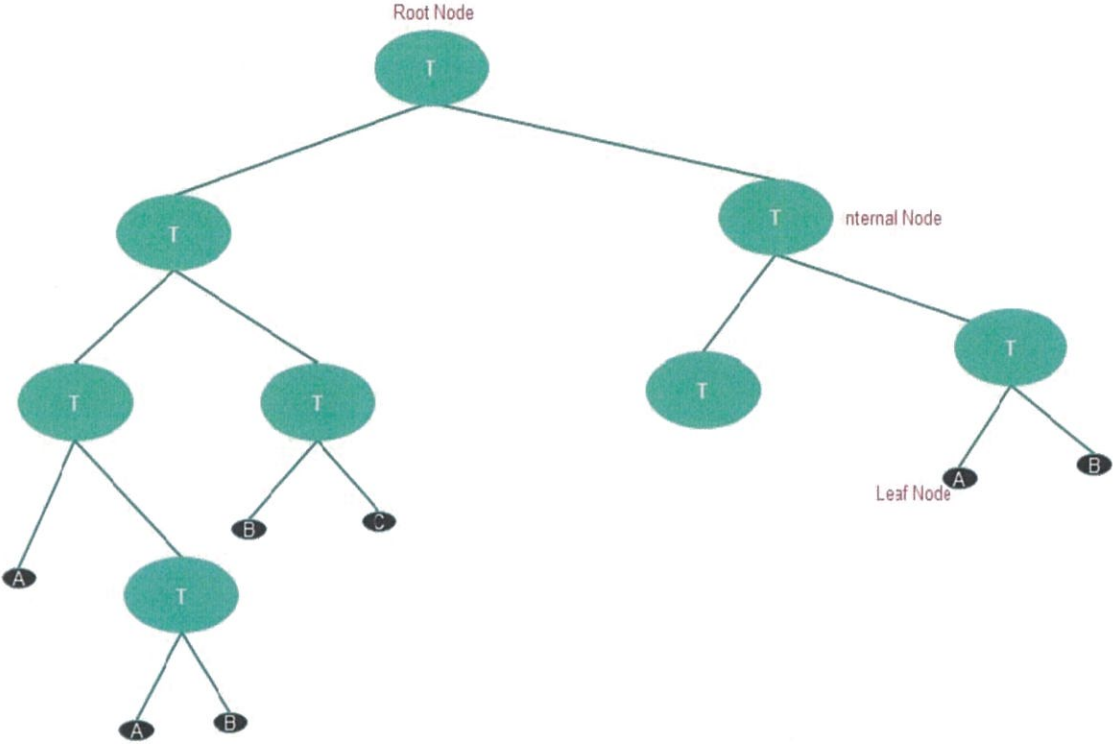


Figure 7. A schematic of the regression model

RF forms a family of methods that consist in building an ensemble of decision trees that are grown from a randomized variant of the tree induction algorithm. This predictor ensemble of decision tree grows in a randomly selected space [36]. Various empirical studies have shown that RF is fast and easy to implement, generates high prediction accuracy, and handles a large number of input data set without the possibility of overfitting. An interesting feature is the built-in possibility of obtaining the unused samples to form estimates of important statistics (out-of-bag estimate) [36]. RF maintains high level of accuracy even with inconsistent data and gives a correlation plot to indicate important variables for the analysis. This algorithm can be used for either classification or regression

model. RF has been classified as a combination of decision trees (classification or regression) with great noise elimination ability that combines weak classifiers of the sample type to produce a strong classifier. It provides an accurate and robust tool for solving many ML tasks ranging from regression, classification, density estimation, manifold learning [37]. Breiman's RF was based on the early work of Amit et al., 1997 which focuses on the geometric feature selection, combined with the random space method of Ho (1998) and the random split selection method of Dietterich (2000). RF method is fast and easy to implement with high prediction accuracy, and it is built with the capacity to handle high volumes of input variables as well as small sample sizes and high-dimensional feature spaces without overfitting. It can be easily parallelized, thus having the capacity to deal with real-life systems. These attributes make it one of the preferred among other ML methods [38-42].

RF operates according to a "divide and conquer" principle by sampling a fraction of input data, growing a tree predictor on each small fraction of data randomly, and then aggregating each predictor.

RF as a robust model can deal with both supervised classification and regression analysis. However, the focus of this research is on the regression analysis. Categorizing RF into classification or regression analysis is based on the desired output for the specified analysis. If the desired output is categorical, RF classification method is used, and the classifier is given by the expression:

$$\psi: X \rightarrow Y \quad \text{where } Y = \mathbb{R} \quad (1)$$

where Y is a finite set of classes denoted by $\{c_1, c_2, c_3, \dots, c_k\}$.

Equation 1 consists of sets of independent variables X and dependent predicted variables Y , such that, depending on the problem type (classification or regression), RF algorithm learns the relationships that exist among variables to categorize into class or predict sets of real numbers. The general framework for the regression model is nonparametric regression estimation in which an input random vector $P \in [0,1]^k$ is observed. For RF analysis, a training data set is of the form:

$$T_n = \{(X_1, Y_1), \dots, (X_n, Y_n)\} \quad (2)$$

For a regression analysis, RF has a predictor consisting of a collection of M regression trees. For the i – th tree in the forest, the predicted value at the split point x is denoted by $m_{M,n}(\mathbf{x}; \Theta_1, \dots, \Theta_M, T_n)$, where $\Theta_1, \dots, \Theta_M$ are independent random variables, $m_{M,n}$ is the regression error estimate, and T_n is the training samples. Thus, the total tree estimate for the forest is the sum of the individual tree estimate that makes the forest. This is denoted by equation 3:

$$m_{M,n}(\mathbf{x}; \Theta_1, \dots, \Theta_M, T_n) = \frac{1}{M} \sum_{i=1}^M m_n(\mathbf{x}; \Theta_i, T_n) \quad (3)$$

The RF in R has a default value of M (number of trees in the forest) to be 500 (that is, $n_{tree} = 500$). Though this value can be adjusted to any arbitrary value higher than the default value. In a classification domain, the RF classifier is obtained by a majority vote among various classification trees and the decisions for classifying the classes is given by equations 4 and 5:

$$m_{M,n}(\mathbf{x}; \Theta_1, \dots, \Theta_M, T_n) = 1 \text{ if } \frac{1}{M} \sum_{i=1}^M m_n(\mathbf{x}; \Theta_i, T_n) > \frac{1}{2} \quad (4)$$

$$m_{M,n}(\mathbf{x}; \Theta_1, \dots, \Theta_M, T_n) = 0 \text{ if } \frac{1}{M} \sum_{i=1}^M m_n(\mathbf{x}; \Theta_i, T_n) < \frac{1}{2} \quad (5)$$

From equations 4 and 5, 0 and 1 denote two different classes into which data samples are classified upon satisfying the indicated criteria for the case of binary classification problem, respectively.

However, RF can intrinsically handle multi-class problems. The RF, however, has been modified based on its splitting method and criteria to generate a variance from the basic principles of Breiman RF [43]. This includes the purely RF under which the centered forest is classified as a method of selecting a variable among other variables and performing a split at the center of the variable selected. The tree growing process stops when a full binary tree is reached to give a 2^k leaves for each tree as the process is repeated k times, where $k \in \mathbb{N}$. k is a smoothing parameter of the algorithm. Another modified

model is the uniform RF, which varies slightly from the centered RF as splits are performed uniformly at random over the selected variable among all variables.

The premise of this investigation is fairly simple. Given some set of factors $(\alpha_1, \alpha_2, \dots, \alpha_n)$ in the domain A , we want to predict the outcome of interest, P . Fig. 7 implies the domain of all factors associated with output interest P in descending order of importance. In traditional regression models, a single equation or model is developed to represent the entire data set. This method provides an alternative approach to this, in which the data space is partitioned into smaller sections where variable interactions are better understood. This analysis uses this recursive partitioning, which represents a cell of the recursive partition, to create a tree where each node T in Fig. 7. To each cell, a simplified model is attached. This process is similar to conditional modeling along the tree structure where conditions are met on a particular variable as we move down the nodes. The final split or node is often referred to as the leaf node. In Fig. 7, A , B , and C are each terminal nodes (leaves). The leaf node implies that after this split, further splitting of the data does not give enough explanation of the variance to be considered relevant in describing the output outcome describing P .

Mathematically, we need to find a function $d(a)$ to map our domain A to our response variable P and we need to make an assumption of the existence of a sample of n observations:

$$\beta = [(a_1, p_1), \dots, (a_n, p_n)] \quad (6)$$

β represents samples of n observations that contains independent variable a and output variable p . In equation 6, (a_n, p_n) is the n^{th} sample set of independent variable and output variable, respectively.

According to regression equation's standard, our criterion for choosing $d(a)$ will be the mean squared prediction error given by the expression, $E[d(a) - E(p | a)]^2$. For each of the individual leaf-node l and training samples k in the regression tree, then, our model is given by,

$$\hat{p} = \frac{l}{k} \sum_{l=1}^k p_l \quad (7)$$

In equation 7, \hat{p} represent the sample mean of the response variable considered for each cell which creates a piecewise constant model of the sample and p_l represent response variable at leaf-node l . This feasibility criteria maximizes the decrease in impurity and it is the principal driving statistical mantra behind regression analysis using regression tree.

Implementation of the IHA is primarily carried out through R statistical software and is somewhat easy to execute. The dataset for the implementation that comprises the P-S-P-P space were imported into R statistical environment. These datasets were a simulation results from a MATLAB code that implement the microstructure evolution model and surrogate model to generate dataset at each sub-space of the material and product design [2]. As a set-based design problem, ranges and resolutions for the independent and dependent variables are as stated in Tables 1 and 2.

Predicted ranged data set was imported into the R programming and RF algorithm was initiated. The mapping from the processing stage to the structure stage generated some sets of data. The mapping model in this stage was considered by varying the independent variables from the minimum to maximum ranged values by considering respective resolutions. The mean, maximum, and minimum response of the output space was computed. The deviation analysis was carried out for each of the generated output datasets at the processing-structure stage. The data sets consist of 42,631 observations and 10 variables. The datasets were seeded to ensure that RF generate same results when the same model specification is run at any time. Randomly-sampled indices were created for the data frame to avoid overlapping subset of indices. The model was fitted to random subsets of input dataset. This process was again conducted for the property-performance space to generate feasible solution space at the performance stage.

For this analysis, previous research was used as the basis [2]. The deductive design process is performed hierarchically from inductive and goal-orientated analysis along the Processing-Structure-Property-Performance (P-S-P-P) relation (refer to Fig. 1 for details). The model structure at the design space consists of deformation holding temperature, processing time, and cooling rate. These design variables were mapped onto the structure space by mapping functions as expressed in [2]. These processing parameters induce microstructure evolution (Austenite Grain Size (AGS), Ferrite Grain Size (FGS)) in the structure space as the holding temperature and deformation time affects AGS while the

cooling time together with holding temperature and processing time affects FGS. The structure space was mapped onto the property space through the mapping function (AGS and FGS) to evolve the Ultimate Tensile Strength (UTS). The mapping process was repeated for the structure space through the mapping function between the structure and performance space to evolve the FS in the performance stage of the model analysis. The design exploration ranges and constraints parameters for both dependent and independent variables for each model are summarized in Tables 1 and 2.

Table 1. Dependent Parameters for IHA

Model	f1	f2	f3	f4
Parameter	dy (AGS)	$d\alpha$ (FGS)	UTS	FS
Range	[0, 150] μm	[0, 40] μm	[200, 600] MPa	[0.0, 10]
Resolution	5 μm	2 μm	25MPa	0.5
Constraints	N/A	N/A	N/A	≥ 2.0
Module	1	1	2	3

Table 2. Independent parameters for IHA

Parameter	T [K]	t [sec]	CR [$^{\circ}\text{C}/\text{sec}$]	h_i [mm]
Range	[800, 1400]	[0.0, 8.0]	[0.0, 3.0]	[25, 40]
Resolution	50	0.2	0.2	0.5
Input Model	f1-f3	f1, f2	f1	f4
Input Module	1, 2	1	1	3

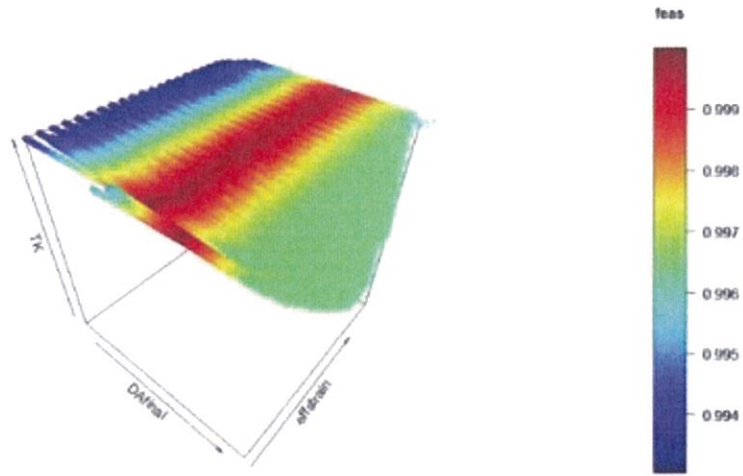
An iterative simulation procedure for bottom-up process-flow together with top-down guidance from system performance requirements is essential to providing the possibility to parallelize the deductive (bottom-up) simulation and to accomplish ranged sets of solution that must be selected through the top-down strategy in the design space (Choi et al. [4][5]). The objectives of the IHA are (a) to explore top-bottom, system requirements control design, guiding the deductive modeling and simulation and (b) to be able to manage uncertainty hierarchically in the model chain, P-S-P-P relation.

2.4 Results and Discussion

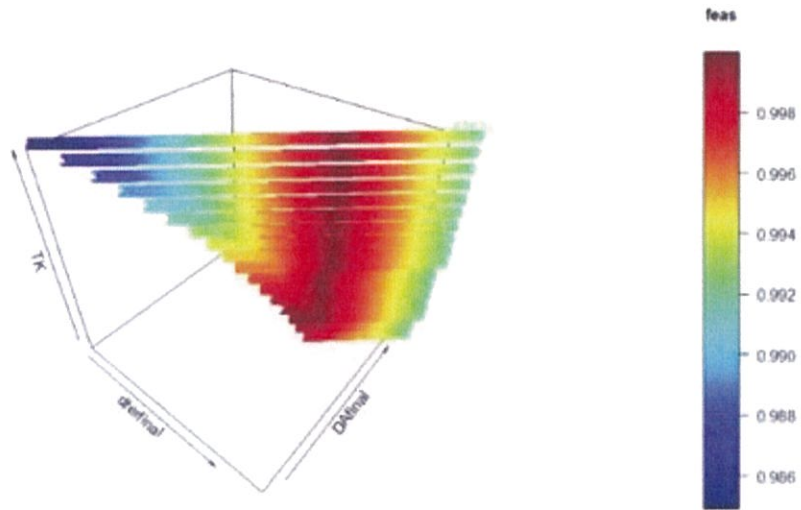
The MATLAB simulation for generating dataset in considering the forward modeling (Deductive simulation) is not computationally expensive as the P-S-P-P linkage was hierarchically examined. Ranged set of data were generated by considering model mapping function at each stage of the deductive design process to finally generate the dataset in the performance space. The dataset was imported into R statistical environment for further analysis. At each stage of the P-S-P-P linkage, feasibility check was carried out by considering the ANOVA method which is determined by the relationship between the mean of the output vector and the output variables in R programming.

It was observed that at each iteration stage, after considering feasible solutions, dataset reduced in population size. This validates the reduction in propagated uncertainties associated with multiscale material design process. Figures 8 and 9 below indicate the 3D plots of the forward modeling of the IHA process. These plots show the variation of data points from the normalized mean. On the legend, the dark-red portion of the plot indicates highly feasible points while the blue portion indicates the less feasible region. As the value of the fea is increased, the robustness of feasible points in the design is better refined because predicted feasible design points are closely located in the mean point.

In IHA, we can regulate the design problem space by specifying upper and lower bound in the performance level. This approach leads to the top-down design analysis as shown in Fig 1. It allows the designer to determine the value of the processing variables that meet the required performance need for a product. The performance space is constrained in the inverse simulation and modeling by specifying the lower and upper bound.

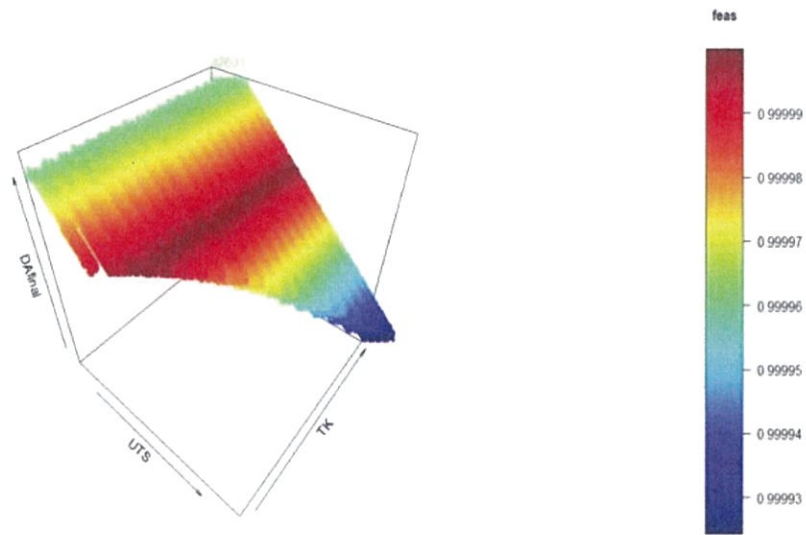


(a)

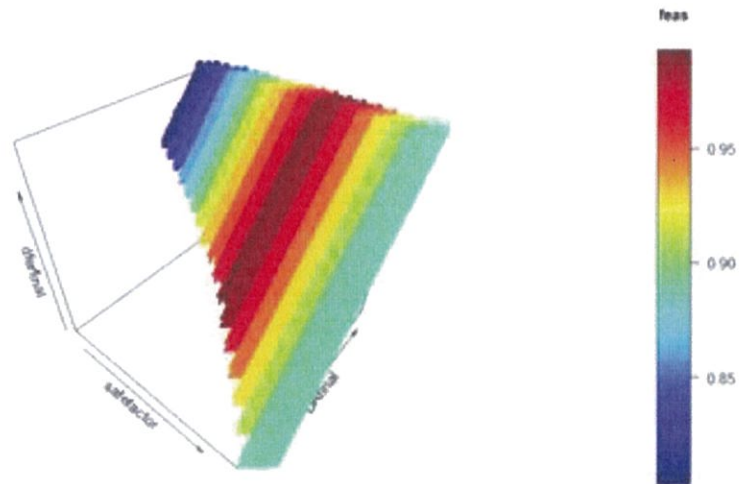


(b)

Figure 8. Feasible regions indicating desirable design spaces in (a, b) Structure spaces (AGS, FGS)



(a)



(b)

Figure 9. Feasible regions indicating (a) Property space (UTS), and (b) Performance space (FS).

Ranges of data set are derived for the performance space by considering selected resolutions and the assigned constraints. The ANOVA model was implemented in the RF algorithm and Tables 3 and 4 show feasible solution set for the forward and inverse modeling below.

Table 3. Feasible ranged solution set for the forward modeling

Parameters	AGS	FGS	UTS	FS
Feasible Range	84.68-84.9	32.54-32.84	193.169- 193.1818	1.578- 1.676

Table 4. Feasible ranged solution set for the inverse modeling

Parameters	TK	AGS	FGS	UTS
Feasible Range	1340-1360	84.41-84.70	32.61-32.69	193.171- 193.174

The accuracy of the model to map the design spaces without propagating errors across multistage was observed by computing the Root Mean Squared Error (RMSE). The model gave RMSE value of 6.665×10^{-5} . This value indicates that there was negligible propagated error across the modeling analysis. This is in good agreement with the robust nature of the process which helps in reducing or eliminating errors associated with multiscale material modeling.

2.5 Closure and Future work

The ANOVA model was introduced in this analysis as a mapping metric in using a ML approach to determine feasible solution points considering material and product design along the P-S-P-P stages. This analysis shows the robustness of RF as an ensemble of multiple decision trees to compute the feasibility in a multiscale deductive and inductive analysis for material design. This method reduced the computational time in simulating the algorithm to a very great extent. This will reduce the processing time for a designer to come up with required material that meets specified constraints.

In conclusion, RF suggests a practical robust design problem across different design scales.

Future work is focused on modeling of the TTT curve by the application of the developed model as it is essential to validate the approaching methods. TTT curve is a transformation diagram used to analyze the microstructure behavior of steel as it undergoes

isothermal processes. An understanding of TTT is required to influence the microstructure as well as the mechanical properties in the final product (steel). The TTT diagram shows the phase transformation represented over a wide range of temperature variation with time for a particular steel composition and its austenite conditioning. It also includes the transformation start and finish temperatures, phase stability regions, and hardness values. The traditional way of determining a TTT diagram is time consuming and difficult. This involves the use of dilatometer, microstructure characterization and hardness testing. There are extensive literatures concerned the transformation of steel but only a few is given for the prediction of the transformation diagrams.

Chapter 3

A Predictive Machine Learning Approach to Time Temperature Transformation Diagram Modeling in Materials Design

3.1 Introduction

Steel and its complex transformation behavior have witnessed continuous interest since the start of the iron age. The increased interest originates from the technological advantage steel transformations present, such as longer lasting roller bearings, stronger and tougher swords, safer cars, higher windmills, etc. This interest has led to progress in both technological and scientific knowledge.

The technological knowledge is represented in the vast knowledge available on the characterization properties, processing of steel types, properties of steel resulting from these processes, and for a specific application, which properties of steel are required. The scientific progress is demonstrated in the vastly available knowledge in the constituents of steel, its microstructures, deformation mechanism, kinetics of atoms, surface chemistry, etc. Scientific effort has been harnessed to explain technological knowledge in terms of fundamental physical principles only.

Currently, this approach has yielded knowledge that influences the exploration of new approaches in steel technology, yet current knowledge solely based on physical principles cannot give accurate predictions for steel transformation behavior due to its complex nature.

3.2 Literature Review

The complexity of the steel transformation behavior follows from the simplest physical analysis of the transformation process. Steel is made of iron and carbon constituents with some other alloying elements. Pure iron in equilibrium has a ferrite structure whose crystal structure is Body Centered Cubic (BCC) at room temperature and pressure and Face Centered Cubic (FCC) crystal structure known as Austenite at a temperature between 912°C and 1394°C.

Most low alloy steels have the same equilibrium phases, though at different temperatures. These phases depend solely on chemical composition since phase transformation are controlled by the changes in free energy of the phase involved. In

addition, the thermodynamics determines the reaction heat of a phase transformation. Depending on the amount, type, and combination of alloying elements, the free energies of the FCC and BCC phases change significantly. In some cases, the effect of an element is even reversed when another element is added, resulting in the formation of other phases in combination with carbon, iron, or other elements.

The thermodynamics of steel structure determines the driving force for phase transformation, and the phase that actually forms is determined by the kinetics of the phase transformation. Thus, the transformation kinetics greatly influence the resulting structure and properties of steel. During cooling, diffusion of alloying elements occurs, and this results in local composition variations. The rate of diffusion is affected by temperature and the free energies of the occurring phases. If the time of diffusion for equilibrium phase transformation is insufficient, metastable phases are formed such as Bainite, Cementite, Pearlite and Martensite. Steel consists of crystal structures with different orientations at the microscopic level. The size, shape, and distribution of these structures have a large influence on the kinetics of phase transformations of steels. To fully describe the kinetics of steel transformations, the thermodynamics of the non-equilibrium phases must be known. Also, one needs to know the diffusion coefficients of all alloying elements as a function of temperature, local composition, and structure, which are all difficult to measure. This difficulty encountered using traditional method of steel modeling has led to new statistical approaches in steel technology.

3.3 Design Approach

In this work, statistical modeling was employed to model the TTT curve. This method is an alternative to physical modeling which is very complex as outlined in the previous section. A common approach to physical modeling is to use some sort of differential integral over independent parameters valid for small volumes of steel.

Thermodynamic properties from an extensive database are currently being used to determine the effect of composition on the driving force and other thermomechanical processes associated with the transformation of steel systems involving two or three common alloying elements. Generally, steel alloys contain 5 to 15 alloying elements. This makes a physical approach too complex for now.

We consider the task of predicting temperature transformation diagrams as an approximation problem by obtaining a model with known data. For this reason, we describe each curve, which indicates the start or end of a microstructural transformation, with the function

$$T = f_i(\text{time}) \text{ where } i = 1. \dots n \quad (8)$$

where T is the transformation temperature in degree Celsius, time is the time of initiation or completion of a microstructural transformation, $f_i(\text{time})$ is the mapping function that defines the relationship in equation 8 at each phase, and n is the number of phase transformation.

This model is developed using RF algorithms incorporated with Monte Carlo simulations. The schematic diagram of the Monte Carlo algorithm is shown in Fig. 10. One of the challenges faced with ML approach is the limited data available for modeling. The accuracy of ML technique relies solely on the robustness of the model. The larger the dataset, the more robust the analysis and the more accurate the predictions will be. To deal with this staggering challenge, several methods have been implemented to improve the accuracy of ML techniques.

For our analysis, Monte Carlo simulation was implemented to deal with uncertainty propagations that arise from model parameter ambiguities. Model parameter uncertainties are associated with design variables or control factors as a result of incomplete knowledge of model parameter/input. Monte Carlo simulation performs a random sampling and conducts large number of simulations in order to observe the statistical characteristics of the model output. For an experiment, the possible input random variables $X = (X_1, X_2, \dots, X_n)$ are sampled according to their distribution function. Then the values of the output variables Y are calculated through the performance function $Y = g(X)$ for the random sample input variables. With several experiments performed in this manner, sets of output variable samples are obtained for the statistical analysis used to estimates the characteristics of the output variable Y . The simulation process of the Monte Carlo simulation is depicted in Fig 10. Three steps are required in the process: Step 1 involves sampling on random input variables X , Step 2 involves evaluating the model output Y , and Step 3 is performing statistical analysis on the model output.

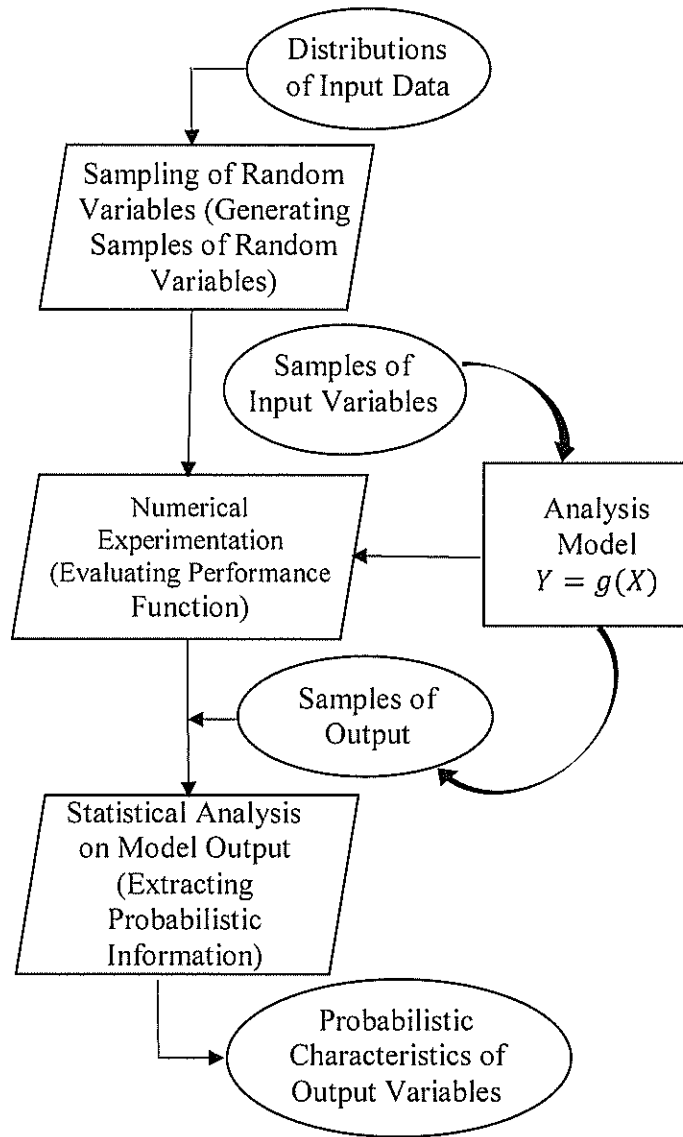


Figure 10. Schematic diagram of the Monte Carlo Algorithm

The chemical composition of A8 steel is shown in Table 5. The constituent materials and their percent compositions are the factors that determine its mechanical properties for its application to dies, punches, drift pins, pneumatic tools, hammers, chuck jaws, hot-rolls, etc. A8 steel has a very good toughness, wear resistance, and excellent dimensional stability in heat treatment. These attributes make A8 steel an excellent choice for applications that require higher toughness than that of high-Carbon or high-Chromium steels. It also has better wear resistance when compared to shock-resistance steels.

Table 5. Chemical composition of A8 Steel

Material	C	Mn	Si	Cr	Mb	Tn
% Composition	0.55	0.30	0.95	5.0	1.25	1.25

The carbon content in the A8 steel significantly helps in austinite and martensite phase formation during microstructural transformation, which helps to improve the mechanical strength and hardness respectively. In general, alloying elements have been found to influence the transformation kinetics and mechanisms in which carbide forming elements such as Molybdenum and Chromium produce tremendous changes in the isothermal transformation process.

The formation of austinite structure and the ferrite structure has been generally seen to be the major transformation phases effected by alloying constituents [44]. Austinite grain size, alloying elements, which tends to slow the transformation reaction, and carbon content has been found to be the major contributors to the hardenability of the steel. The steel is hardened when it is transformed from austinite phase to martensite upon quenching. As the steel is cooled, microstructural transformation from austinite to martensite occur. The martensite phase stops at a temperature where pearlite, and eventually ferrite microstructure, emerges in fine grain steel. This causes a reduction in grain size, and, thus, there is a shift in the TTT diagram towards the left. Increase in percentage of carbon lowers the martensite start temperature, causing a shift in the curve towards the right is observed [45].

For this analysis, we collected a TTT diagram for A8 steel in graphical format. The statistical approach to modeling the TTT curve is only able to process numerical information. Therefore, the TTT diagram needs to be converted into a numerical format. Numerous conversion methods can be utilized, but the one used for this model is an intercept method. In the intercept method, a number of fixed test lines is drawn over the diagram. The intercepts of these lines with the phase boundaries in the Continuous Cooling Transformation (CCT) diagrams determine the coordinates describing the diagram. An advantage that the intercept method has over the grid method is that the diagram can be represented by a relatively small number of data points since the data points are at the

relevant phase boundaries instead of the entire phase region. These data were imported into MATLAB for Monte Carlo simulation. The Monte Carlo simulation uses Probability Distributed Function (PDF) to analyze and generate random samples as depicted in Fig. 10. 80% of the random output variables were then used to train our RF model while the remaining 20% was used to test our model.

3.4 Results and Discussion

From the generated datasets for the TTT curve, the measured time and corresponding temperature values were imported into MATLAB for the Monte Carlo simulation. To carry out Monte Carlo simulation, the constitutive equation is required for numerical experimentation. This is the analysis model in which the performance function is evaluated to generate samples of output variables. Monte Carlo simulation was to generate 100 random data samples as shown in Fig. 11 before applying the analysis model.

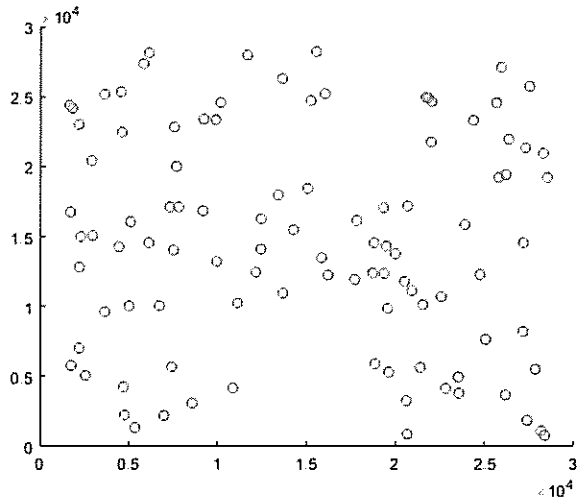


Figure 11. Random data sample generated with Monte Carlo simulation

The applied constitutive model together with the uniform distribution function in MATLAB was used to extract probabilistic information from output data samples. In order to determine the constitutive equation for the TTT plot, several analyses were implemented in MATLAB to generate the best curve fit from the measured datasets. The best method was achieved by dividing the TTT dataset into two sections, the upper bound and the lower bound, as shown in Fig. 12 and 13, respectively.

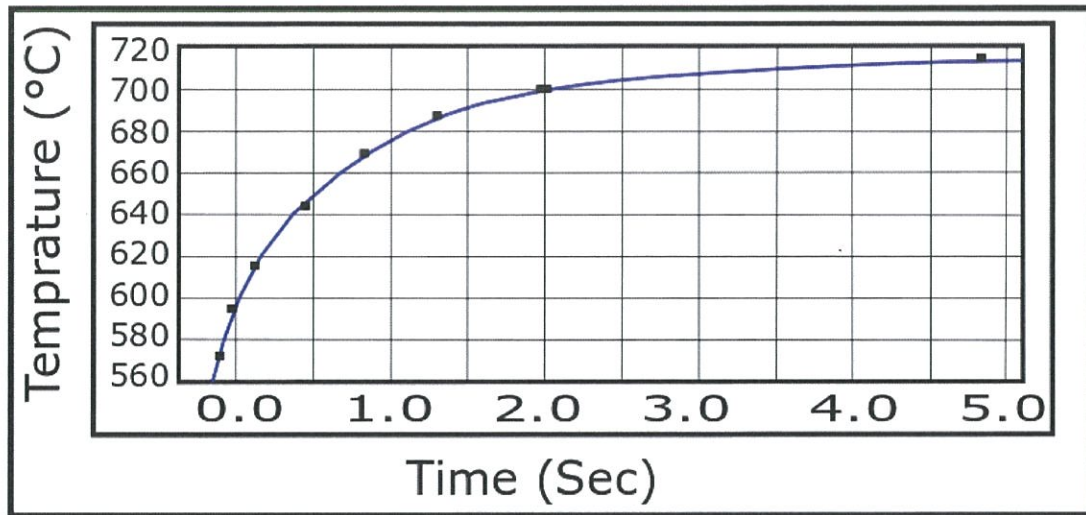


Figure 12. Upper bound plot with Monte Carlo method

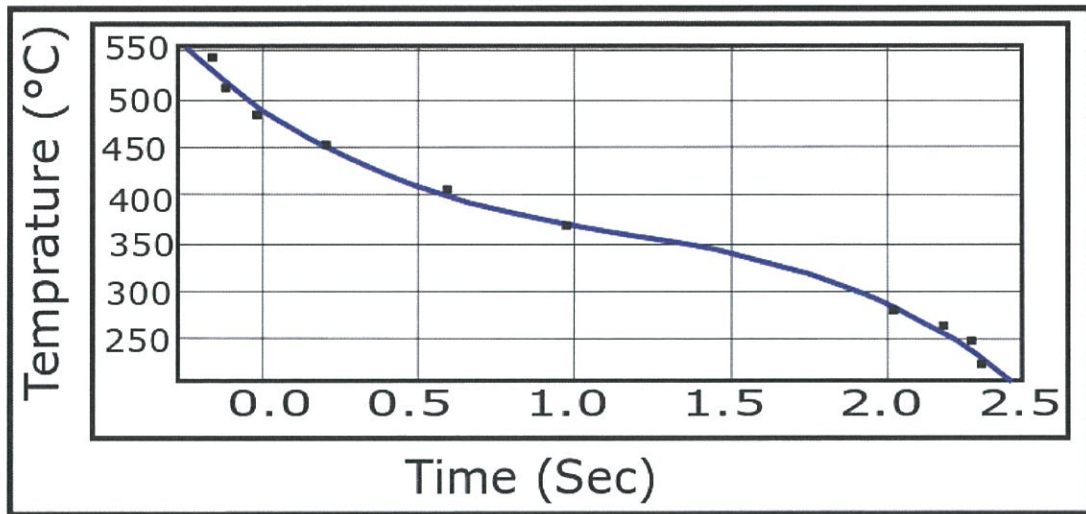


Figure 13. Lower bound plot with Monte Carlo method

The final TTT curve was achieved by super-imposing the two halves as seen in Fig. 14. The best fit for the upper bound after several manipulations is the power function with the number of terms at 2. For the lower bound of the CCT curve, power function with 2 number of terms was found to give the best fit with an R-square value of 0.999 and a 95% confidence interval as shown in Fig. 13.

The above-mentioned process analysis helps in determining the constitutive equation to model the CCT diagram. For our case, two different equations were derived for the Monte Carlo simulation. Monte Carlo algorithm was implemented at this point after modifying the open source code to suit our analysis. To test the correctness of the constitutive equations, 100 simulations were performed, and the plot in Fig. 14 below shows the generated datasets and the TTT curve. This plot clearly shows the superposition of the upper and lower bound. This plot is similar to the one generated with measured data.

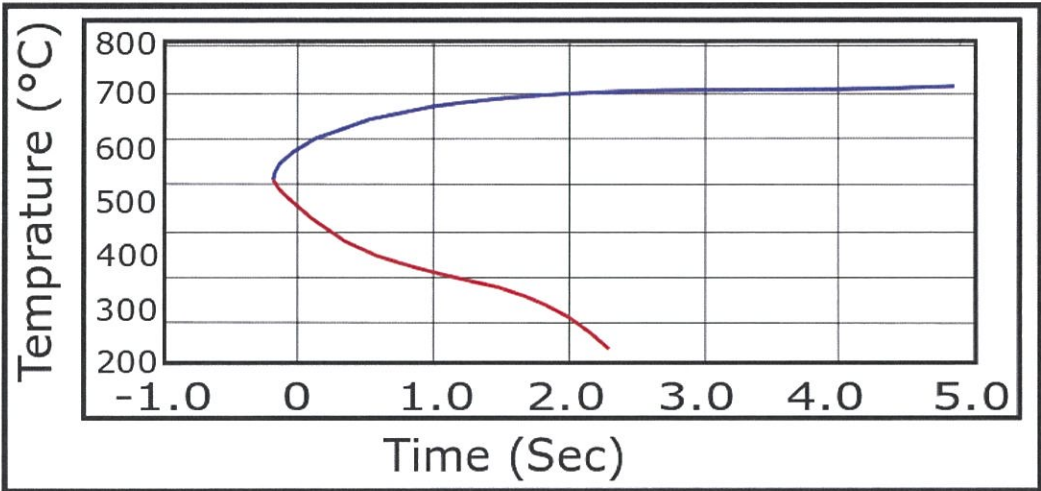


Figure 14. Super-position of the upper and lower bound plot

The output of Monte Carlo analysis was imported into R-statistical environment for regression analysis. The RF model was trained with 90% input sample, and a 10% test data sample was used to analyze how well our model performed. A Mean Square Error value of 12.5% was derived from the model. The model gave a RMSE of 9.5%. these values indicated that our model predicted values are very close to the actual data set. To validate our model, data points from a previous study were used as an input data for Monte Carlo simulation [45]. The output data from Monte Carlo was imported into R code. The input data was fitted to the RF model, and further statistical analysis was carried out to determine the performance accuracy of our regression model. Figure 15 shows the plot of the TTT curve predicted by the proposed approach. The model gave a very good prediction of the TTT curve with an accuracy matrix of approximately 93%, and it indicates that the model accurately predicts the TTT curve.

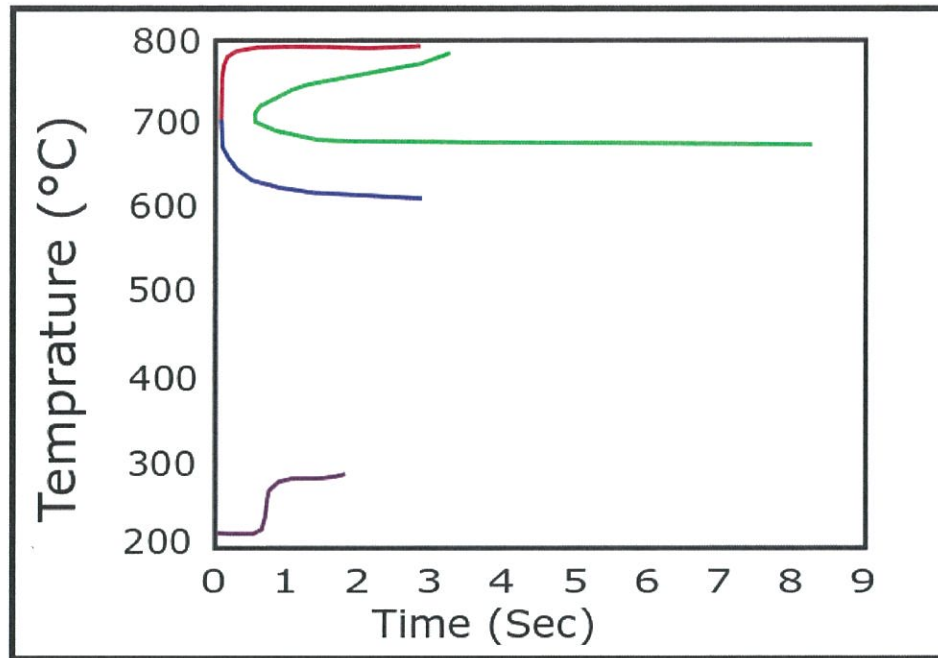


Figure 15. Plot of TTT diagram with RF model

From Fig. 15 plot, deduction of how the cooling rate affects the transformation of austinite into a range of possible phases can be made. The transformation of austinite begins at approximately 788 degree Celsius for this steel. This is indicated by the red curve. The direction of the curve indicates a temperature drop with time. Because the transformation from a phase to another takes time, TTT diagram shows two lines to indicate the start and the finish of the transformation. As the process continues, a point is reached where a new phase emerges. This region is known as the nose of the curve indicated by the region between the end of the red curve and the start of the blue curve. At this point a pearlite and bainite structure begins to form at a temperature between 700 degrees and 670 degrees. The nose is the result of superimposition of two transformation noses as shown in the plot. The upper portion of the nose signifies pearlite structure while lower bainite forms at a lower temperature but above the Martensite temperature. The formation of martensite is observed as the transformation process continues with time at about 220 degrees. This phase increases with decreasing temperature and does not change with time. The transformation is athermal in nature at this point. That is, the transformation process is completed in a short time.

3.5 Closure and Future work

TTT diagram of cold working steel A8 steel that contains the microstructural changes during heat treatment was observed in this thesis. Digitized diagrams from the previous study were used as input data for Monte Carlo simulation [45]. Monte Carlo simulation provides a framework for model robustness and deals with uncertainty propagation due to limited data set. Monte Carlo simulation was used to generate 100 data samples using probability density function. RF algorithms gave a prediction accuracy of 92.7%. This shows the prediction ability of the RF method to handle large variable spaces and run efficiently on large data bases without variable deletion. From the results, our regression model gave a good prediction of the curves.

However, our model prediction accuracy is limited to the type of steel to which it was trained. Use of different steel types could give a poor prediction due to the different percentage of constituent elements which affect the mechanism and kinetics of steel transformation during heat treatment. Efforts are ongoing to predict the TTT curves of other cold working steel in order to validate the effect of constituent's elements on the transformation mechanism associated with heat treatment and also to further test our approaching methods.

In conclusion, this analysis shows the application of Monte Carlo simulation together with RF as a robust approach in dealing with uncertainty propagation associated with modeling TTT diagrams and reduced the computational time compared to the mathematical approach to TTT modeling. Future work is geared towards AI implementation to material modeling. Effort will be focused on performing a Finite Element Analysis (FEA) of hot rolling process to validate the IHA method. AI will also be applied to modeling constitutive behavior of Shape Memory Alloy (SMA) due to its interesting properties. Understanding the behavior of engineering materials helps in determining the appropriate design model for various applications and uses.

Chapter 4

AI Adoption to Modeling Constitutive Behavior

4.1 Introduction

Constitutive models have been extensively used to link the state of stress and strain of most engineering materials during mechanical analysis and their behavior in structural components. This is common to all mechanical analysis of engineering materials. Constitutive equations that define the constitutive models are complementary equations to the balance and kinematic equations. It is clear that the physics behind the microscopical phenomena for various materials used in engineering practice, such as metals and alloys, fiber composites, polymer, wood, and concrete differ. However, it is possible to a large extent to employ same principles and concepts in establishing constitutive relations for these different materials. Indeed, the mechanical characteristics of an engineering material are determined by its microstructure. Figure 16 shows an example of microstructures for different materials. Crystalline materials and amorphous materials behave differently as do single crystals in comparison to polycrystalline materials due to variation in microstructural composition.

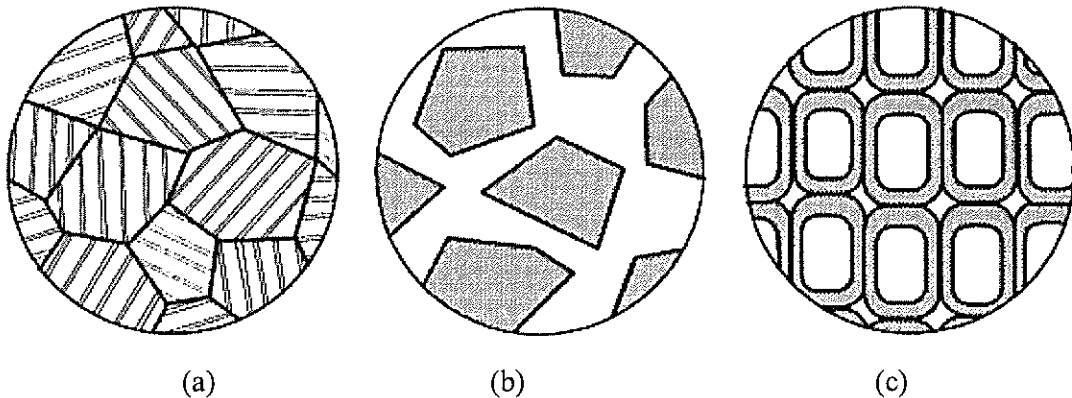


Figure 16. Typical microstructure of (a) Steel with perlitic grain structure and eutectoid composition, (b) Concrete, (c) Wood.

4.2 Literature Review

The mechanical properties of engineering materials are often significantly affected by temperature and loading rate. For example, the ductility of a metal is reduced at a low

temperature and high loading rate. It should be noted that constitutive models are mathematical simplifications and representation of a quite complex physical behavior, and there is no such thing as an “exact” model. For example, it is appropriate to model steel behavior as an elastic-plastic, but it is inappropriate to claim that steel is elastic-plastic. Steels and other engineering materials can be model in a number of ways depending on the purpose and the required precision of the model predictions.

Constitutive models have been developed following conceptually different approaches such as micromechanics or fundamental approach, phenomenological approach, and the statistical approach. The fundamental approach requires a complete knowledge of deformation and failure characteristics to establish a constitutive relation.

This model is obtained through averaging techniques such as homogenization, which can sometimes be carried out analytically. For the phenomenological approach, the model is established directly based on observed characteristics from elementary tests. The calibration is carried out by comparing with the experimental results and/or with micromechanical predictions for well-defined boundary conditions on the pertinent Representative Volume Element. An example is found in the observation of the yield stress of mild steel from a tensile test. The general approach is to optimize the predictive capability of the model in the calibration process. The objective function to be minimized is the measure of the difference between the predicted response and the experimentally obtained data.

The arguments of the constitutive functions are observable variables such as stress, strain, and temperature, in addition to a sufficient number of non-observable (internal) variables that represent the microstructural changes. The statistical approach to modeling constitutive behavior are the least fundamental in that they are established as response functions for specific loading and environmental conditions. This approach involves the application of AI to examine the relation between variables of interest. AI refers to intelligence displayed by machines that simulate human intelligence. It is a broad term for smart machines that can perform human tasks that require cognitive, judgment-based decision making. Several attempts have been made by researchers to use AI technique to model constitutive material behavior.

ML is an application of AI that provides systems the ability to automatically learn and improve from experience without being explicitly programmed. ML focuses on the development of computer programs that can access data and use it to learn for themselves. ANN has been used to model constitutive behavior of concrete [46]. Ghaboussi et al, 1998 presented an improved technique of ANN approximation for understanding the mechanical behavior of drained and undrained soil [47]. An extensive use of ANN has proved that neural-network based constitutive models can capture nonlinear behavior with high accuracy. Javadi et al. developed a code based on application of neural networks in constitutive modeling of complex materials. They use actual material test results to extract stress-strain relationships and to train the model. It has been shown that models trained in this way can be effective in learning and generalizing the constitutive behavior of complex materials and give better results when compared with conventional constitutive modes. It should be noted that AI-based models are empirical models because they make use of experimental data in order to extract information. This, however, limits the intelligence of the AI-based model to the accuracy of the experimental data. AI aims to establish a mathematical relationship between some dependent variable X and an independent variable Y :

$$Y = f(X) \quad (9)$$

The above relationship depicts a simple mathematical expression, but a complex relationship is obtained by using paradigms imitating human reasoning. SMAs, such as Flexinol, are materials that can undergo plastic deformation and return to their undeformed shape when heated. SMAs undergo a crystal transition between a martensite phase and an austenite phase as the material temperature increases [48]. When subjected to low temperature conditions, SMAs display a small elastic modulus and can be deformed rather easily [48]. Some SMAs can also be antagonized to alter their shape when electrical currents are applied, causing appreciable contraction and expansion [49]. Whereas most materials expand when heated, these SMAs can be tempered to contract when an electrical current is applied and return to their original shape after the current is ceased. These SMAs are often fashioned into wires that can be used as mechanical actuators when a current is applied [50]. It is this electromechanical behavior that is of much interest to us. As an SMA

changes its shape, the metallographic transformations from the martensite to austenite phases cause a significant change in the electrical resistance of the material [48][51].

One such SMA is flexinol, a variant of nitinol, which is the most widely used SMA. Flexinol is an alloy comprised primarily of nickel and titanium that was designed to exhibit optimized characteristics for actuation, including an extensive work life, high repeatability, and strength for shape recovery [52]. Nitinol has been extensively studied in scientific literature in order to understand its behavior, but flexinol has not been examined to the same extent. It is known that nickel and titanium-based SMAs can exhibit a recoverable strain of up to 8%, but it is recommended that the strain not exceed 4% of the overall length of the wire to ensure a high number of usage cycles [49]. To design and optimize the applications of the SMAs, a clear knowledge of its behavior and characteristics is required. SMAs possess some thermo-mechanical properties of interest such as Young's modulus and the coefficient of stress influence during austenite-martensite and martensite-austenite. These properties should be determined before its use to various applications. Several methods have been employed to determine the properties of the SMA. Differential Scanning Calorimetry is one famous method used by several researchers to determine the phase transformation temperatures. This method however is only suitable for the powder-form products of SMAs and not the finished-form products such as wire. Other methods include the use of Linear Variable Differential Transformer. This consists of masses stacked together and actuated by an SMA wire positioned vertically. Stresses applied to the wire are varied by adding or removing masses to the set of stacked masses. Other experimental setups use the same approach but with different tensile testing equipment to determine the phase transformation temperature for the SMA.

4.3 Design Approach

In this thesis, we employ the use of AI approach to modeling constitutive behavior of flexinol wire. The SMA used was a flexinol wire from Dynalloy, Inc. The diameter of the wire was 0.02 inch and it has a maximum pull force of 34.94 N. Other properties of flexinol is shown in Table 6.

Table 6. Properties of Flexinol wire

Parameters	Value
Density	6.45 g/cm ³
Specific heat	6-8 cal (mol. ⁰ C)
Melting Point	1250 ⁰ C
Heat of transformation	10.4 BTU/lb
Thermal conductivity	0.05 cal (cm ⁻⁰ C-sec)
Thermal expansion coefficient	
Martensite	6.6 x 10 ⁻⁶ / ⁰ C
Austenite	11.0 x 10 ⁻⁶ / ⁰ C
Electrical resistivity	
Martensite	421 Ohm/Cir Mil Ft
Austenite	511 Ohm/Cir Mil Ft
Linear resistance	0.12 Ohm/inch
Density	6.45 g/cm ³
Specific heat	6-8 cal (mol. ⁰ C)
Melting Point	1250 ⁰ C

The experimental basis for this analysis is can be referenced to previous research [53]. We collected the strain-stress curve at 75°C in a graphical format (see Fig. 17).

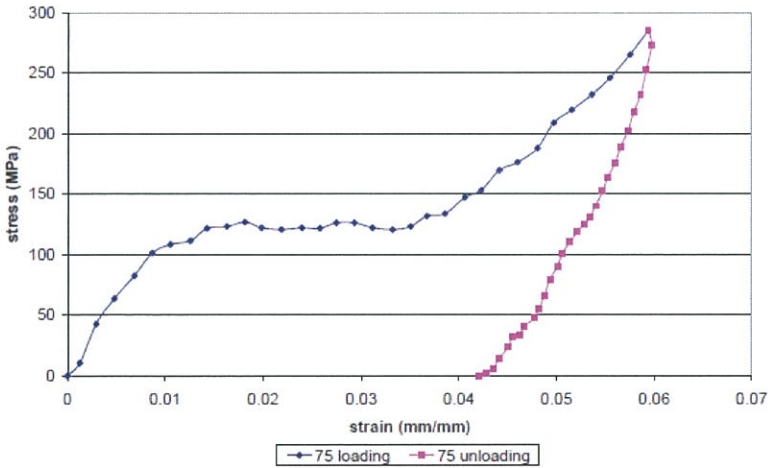


Figure 17. Set data for the set experiment with 75°C temperature applied to the Flexinol wire

The statistical approach to modeling the constitutive behavior of flexinol wire is only able to process numerical information. Therefore, the stress-strain curve needs to be converted into a numerical format. Numerous conversion methods can be utilized but the one used for this model is an intercept method. In the intercept method, a number of fixed test lines is drawn over the diagram, where the intercepts of these lines with the loading and unloading points in the diagrams determine coordinates describing the diagram. An advantage of the intercept method over the grid method is that the diagram can be represented by a relatively small data size. Figure 18 shows a plot of the data points before the application of Monte Carlo simulation

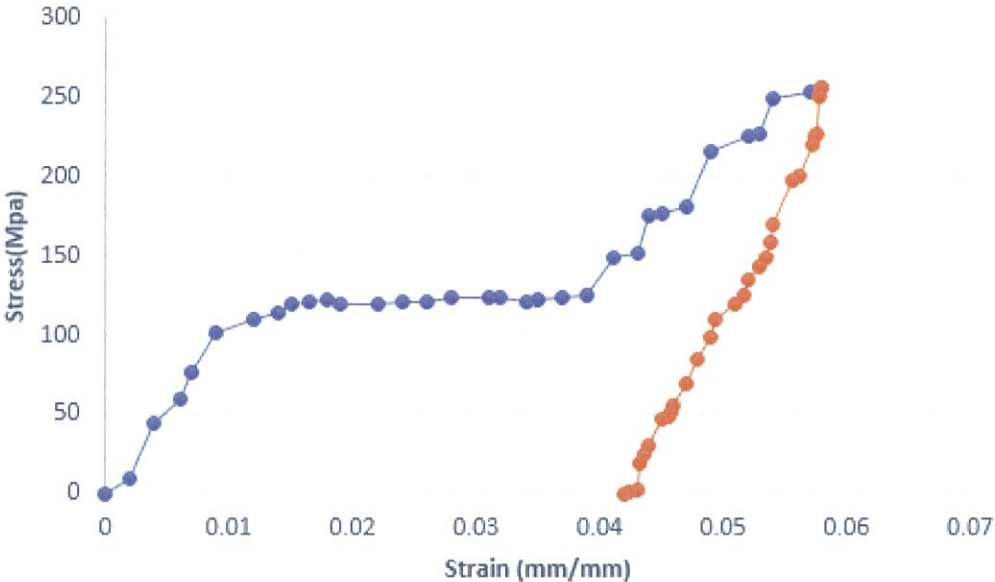


Figure 18. Constitutive behavior plot for Flexinol wire at 75°C using the intercept method

These data were imported into MATLAB for Monte Carlo simulation to generate a plot shown in Fig. 19. The Monte Carlo simulation uses PDF to analyze and generate random samples. 900 data points were generated. The increased number of data points help to improve the robustness of our model and improves the accuracy of the ML technique.

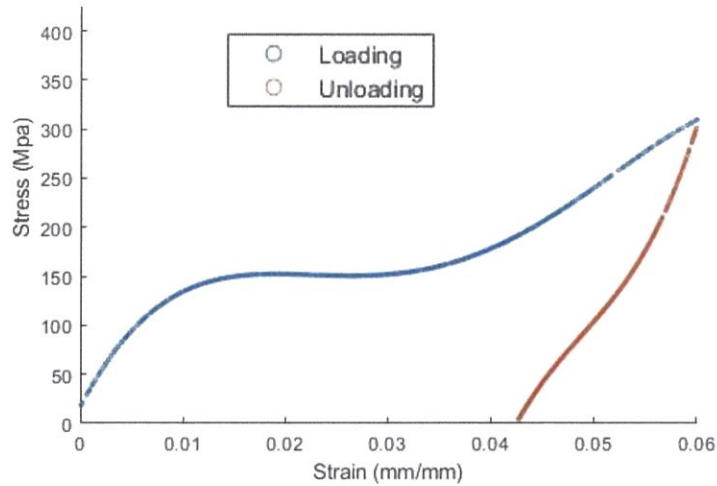


Figure 19. Constitutive behavior plot for Flexinol wire at 75°C after applying Monte Carlo method

RF algorithm was implemented in R statistical environment over the data points and the output variable (stress) was predicted over the input variable (strain). The model gave a very good prediction accuracy of the constitutive behavior of the flexinol wire as Fig. 20 shows the plot of the RF prediction with the data set generated by Monte Carlo simulation. 80% of the random output variables were then used to train our RF model while the remaining 20% was used to test our model. A regression analysis was performed on the data set with 800 numbers of trees.

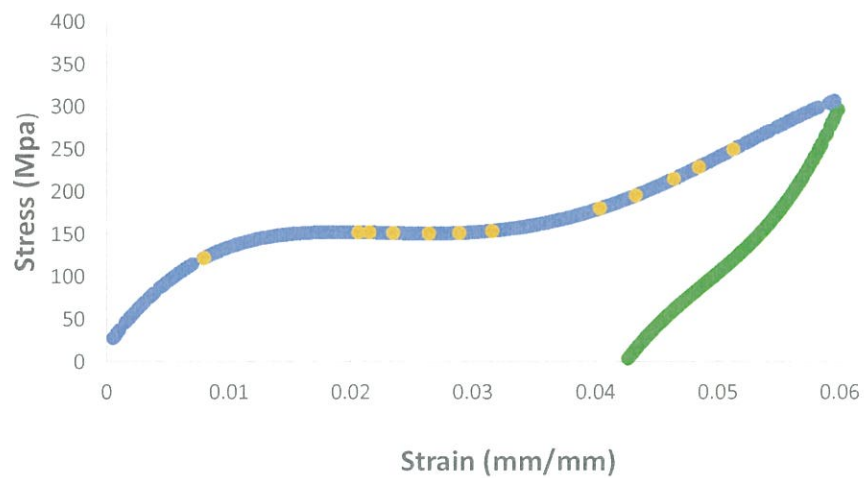


Figure 20. Constitutive behavior plot for Flexinol wire at 75°C consisting of the RF prediction and the Monte Carlo generated data set

4.4 Results and Discussion

From the plot we can observe a close-to-perfect prediction of the constitutive model of the flexinol wire at an operating temperature of 75°C by the RF model. This is expected because the propagated errors associated with the experimental calculation and the error associated with the mapping method to convert graphical information to numerical format has been dealt with by the application of Monte Carlo simulation. With the general knowledge that the AI prediction accuracy is dependent on the accuracy of the input data set, this enables the RF algorithm to give an accurate prediction of the model with a RMSE value of 0.01044 MPa. This value indicates that there was negligible propagated error across the modeling analysis. This is in good agreement with the robust nature of the process which helps in reducing or eliminating errors associated with modeling constitutive behavior using AI.

ML algorithm with the implementation of Monte Carlo algorithm helps to increase the robustness of our model as shown above. AI application to constitutive behavior eliminates experimental cost and time in setting up apparatus for a research aside from eliminating human and associated errors during experimentation.

4.5 Closure and Future Work

AI application to modeling constitutive equation has yielded tremendous progress in material design and modeling. RF approach together with the application of Monte Carlo algorithm has once proven to be a valuable tool for modeling. This work was successful carried out in a R statistical environment together with the use of MATLAB commercial software. Future work will focus on validating the approaching methods using Finite Element Approach. Simplified models will be created, and FEA will be conducted on this model to support research work.

Chapter 5

Validation Using Finite Element Method (ANSYS)

5.1 Inverse Hierarchical Analysis Model for the Hot Rolling Process

FEA has been used as a validation method for most engineering design problems. The engineering capabilities and strength this method brings to engineering design approach has led to the rapid design and development of engineering materials and structures. FEA is a mathematical idealization of a physical behavior for engineering analysis.

In this chapter, the finite element model analysis has been created to validate our analysis model for the IHA for gear design and modeling of the constitutive behavior of flexinol wire. ANSYS commercial software package is used to simulate the roll process design. The rolling process consists of roll passes in between which the workpiece passes before a final product is formed as shown in Fig. 21.

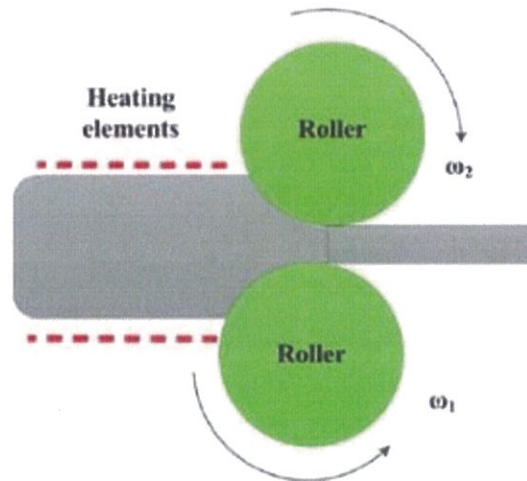


Figure 21. A roll pass design

However, hot rolling process consists of several roll passes in different directions, positions, and depending on the required final products. It is an intermediate process in the gear manufacturing process which plays a significant role in determining mechanical properties of the gear.

A 3D model for FEA was created in ANSYS 19.2. This model consists of two rollers and the heating element (billet). The rollers were made with steel while the billet was made of aluminum. The geometry of the 3D model is as shown in Fig. 22 below.

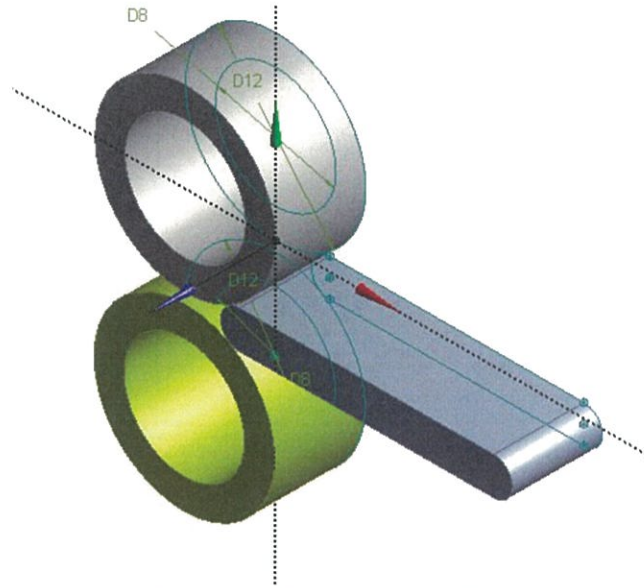


Figure 22. 3D Model of a hot rolling simulation process

Based on the IHA model, the billet height was considered as 25mm and the time step for simulation was set at 2.5 secs and an environment temperature of 1350K was set. The focus of this simulation is to determine the FS which is the output for the IHA. In considering this, the variation of stresses and strain during the deformation process was observed. A non-linear simulation of the model was created with 2.0 mm size of elements and 20 nodes with a quad mesh type on the billet and frictional contact surface between rollers and billet. The rotation angle was set at -180° and $+180^\circ$. At this point, the solution to the defined problem was initialized, but a convergence issue prevented the problem from being solved. The iteration steps could not be completed due to large deformation. To solve this problem, a 2D analysis of the same model was developed in ANSYS. Figure 23 below shows the geometry of the 2D analysis. Due to symmetry, only one roller was used, and the height of the billet was reduced by half. Bottom of the billet was fixed to account for symmetry. All other variables remained constant.

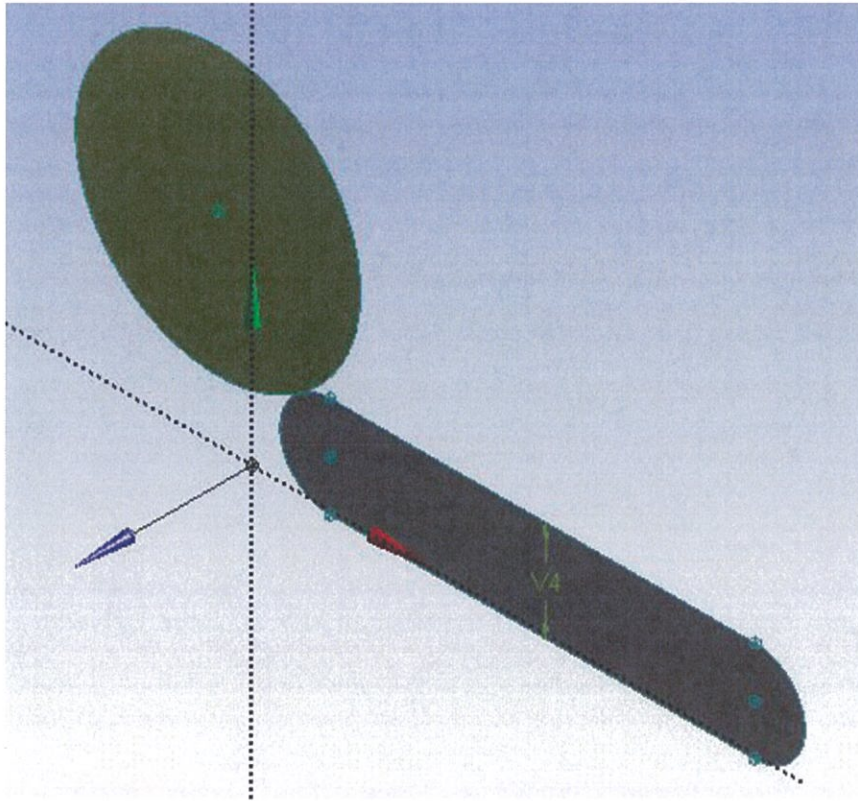


Figure 23. Surface bodies of the 3D hot rolling process

For 2D analysis, the 3D model was transformed into surfaces as shown in the figure above. The initial shape of the incoming billet is a deformable surface with a plain strain geometry which utilizes 2D plain properties. This method helps in overcoming issues faced with 3D modeling of the rolling process.

The solution was initiated after specifying the boundary conditions and the applied loads. The results based on FEA for single roll pass design parameters were compared with the IHA model. Figure 24 below shows the factor of safety plot as the billet underwent plastic deformation after passing through the roll. From IHA method, the prediction of feasible factor of safety ranges from 1.578 to 1.676 while the FEA solutions are between 0.25664 and 15, with 15 being the maximum value. A close observation of the FE analysis indicated that during the rolling process factor of safety that ranges between 0.25664 and 2 were generated along the deformed billet as it passes through the roll.

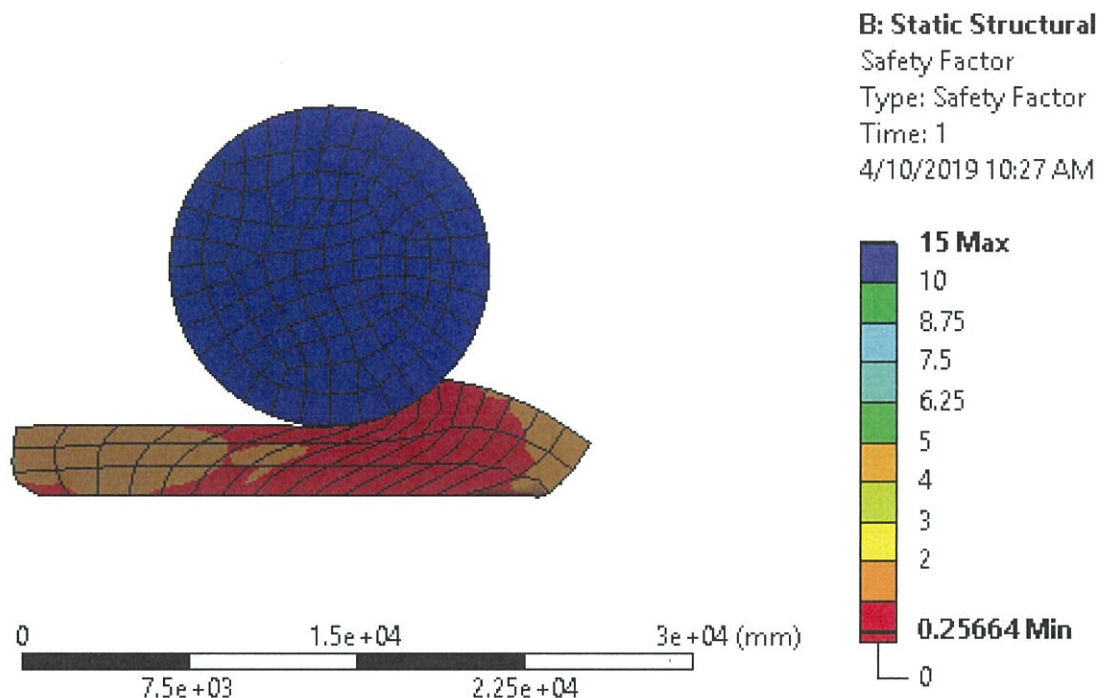


Figure 24. Factor of Safety Simulation Results

By comparing FE results with IHA method, it should be noted that variables at the processing (height of billet, time) stage and the property stage (UTS) were used as input data for this analysis. Table 7 and 8 below shows the FE results and the IHA result.

Table 7. Performance variable evaluation by FE Analysis

Processing (Time, height, TK)	Structure (UTS)	Performance (FS)
2.5secs, 12.5mm, 1350K	193.170	0.25664- 2.0

Table 8. IHA predicted values across P-S-P-P structure

Parameter	AGS	FGS	UTS	FS
Feasible range	84.68-84.9	32.54-32.84	193.169- 193.1818	1.578-1.676

5.2 Constitutive Model Prediction of a Flexinol Wire

For the constitutive model validation, ANSYS 19.2 workbench was implemented. The focus is to simulate the loading and unloading stress-strain curve of the flexinol wire predicted by the approaching methods developed in this thesis. A 3D model with a fixed boundary condition at one end and a displacement condition applied on the other end, as shown in Fig. 25, was developed in Ansys workbench. The model was dimensioned to 1 mm x 1 mm x 1 mm.

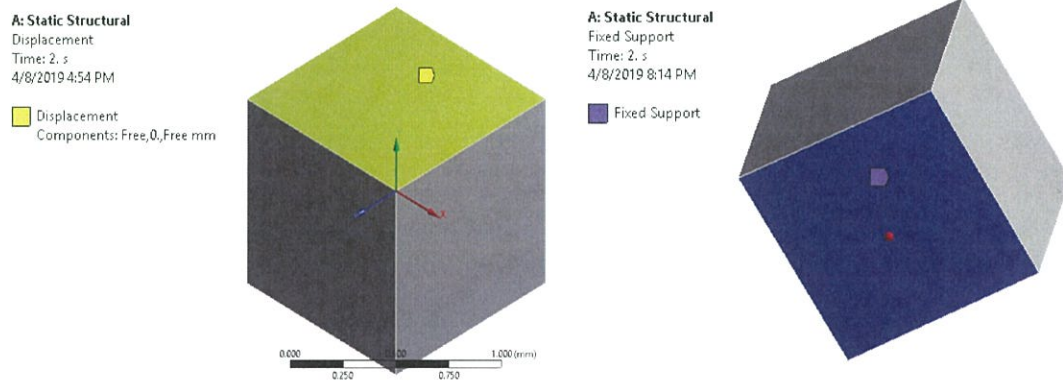


Figure 25. 3D constitutive model for flexinol with boundary conditions

This cube was meshed with one element, and a bi-linear kinematic hardening function was specified for the material with a yield strength of 250 MPa and a tangential modulus of 0 MPa. Three sides of the cube were set on symmetry and a displacement was placed on the vertical surface to control the loading and the unloading process. The equivalent stress and equivalent strain were plotted to generate the stress-strain curve by modifying the chart function in Ansys as shown in Fig. 26 below.

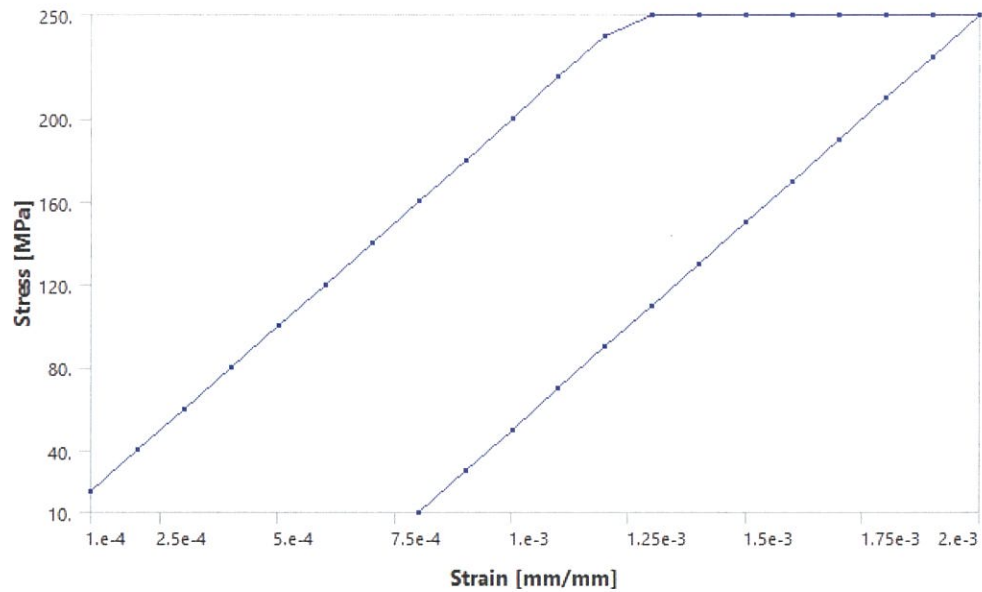


Figure 26. Stress-strain curve of a material modeled after flexinol material properties

Comparing the FE results with the RF prediction, the finite element material model behaves linearly at a stress value of 24 MPa and strain value of 0.0004mm/mm until it reaches the elastic limit of 250 MPa. Plastic behavior of the material is observed at this point between a strain value of 0.00125 mm and 0.002 mm before unloading process begins. The RF model shows a linear behavior at a stress value of 24 MPa and a strain value of 0 mm/mm until it reaches 160 MPa. Plastic behavior is observed from this point to a value of 320 MPa between a strain value of 0.024 mm/mm and 0.06 mm/mm. There is quite a significant variation in the strain values along the plot diagrams. However, the stress values are much in agreement except for the start of plastic behavior. The constitutive model from experiment shows a linear behavior of flexinol starting from 0 mm/mm strain and 0 MPa stress. The material experience plasticity at 120 MPa until it reached a value of 280 MPa within 0.02 mm/mm to 0.04 mm/mm. These results are tabulated in Table 9 and 10 below.

Table 9. Elastic behavior of different constitutive behavior models

	FE Model	Random Forest	Experiment
Stress	24	24	0
Strain	0.0004	0	0

Table 10. Plastic behavior of different constitutive behavior models

	FE Model	Random Forest	Experiment
Stress	250 to 250	160 to 320	120 to 280
Strain	0.00125 to 0.002	0.024 to 0.06	0.02 to 0.04

These plots from the FE model can be compared to the model predicted by the RF method as well as the experimental analysis model, though with some varying differences. These differences are as a result of several factors not implemented into the FE simulation. For example, the geometry modeled as flexinol wire and the operating temperature for the experimental simulation was not considered in this case. This could have a significant change in the behavior of the SMA and will rather require a more complicated simulation to the simplified FEA created.

Chapter 6

Closure and Future work

ML application in computer integrated material design and modeling has been extensively developed. A RF regression model has been developed to map design spaces across the PSPP level in a hierarchical order. This research is characterized with how ML models can be incorporated into the material design and modeling for predicting the material properties of steel used for gear manufacturing. This has led to the development of a working hypothesis and five major tasks. By completion of these five tasks, the final objective can be reached.

Chapter 1 introduced the research by giving an overview, challenges faced, and methods that have been applied to eradicate issues associated with material design. Chapter 2 emphasized on the approaching method applied to material design. As a computational method, the structures of RF and IHA were extensively explained and the feasible solutions were mapped across the PSPP linkage. The prediction accuracy of this model was also examined.

This work was extended further to predict the TTT curve for A8 steel in Chapter 3. A Monte Carlo algorithm was implemented with the RF model to deal with uncertainty issues associated with limited data set and the propagated error associated with the digitization of graphical information, which is a major problem faced in the data world-domain. Because the predictive capability of an AI method depends solely on the accuracy of the data set, Monte Carlo implementation helped with the generation of more data points. This improved the robustness of the RF model.

In Chapter 4, the constitutive behavior of a flexinol wire was examined with the implementation of the developed model. This is important because of the role that constitutive behavior plays in understanding mechanical characteristics of materials. This is a major factor in material design and modeling. The model gave a very good prediction with an RMSE value of 0.01044 MPa.

To validate the approaching method used in this research in Chapter 5, FEA of the hot rolling process was carried out with ANSYS. ANSYS is a FEA tool used to simulate engineering problems and deliver product modeling solution with unmatched scalability

and comprehensive multi-physics capability. With a simplified model of a single roll pass and a billet of known geometry, as shown in Chapter 5 of this thesis, FS was computed based on simulation. The FEA range of FS was 0.2566-2.0 while the result predicted by the RF model was 1.578-1.676. This shows that the FEA results and the prediction of RF model are close with a percentage variance of 19.3%

Also, the constitutive behavior of a flexinol wire was modelled using ANSYS as a validation method. The FEA model shows comparable results with the output of the approaching method employed in this research. The AI application to constitutive behavior modeling shows greater improvement in modeling constitutive behavior of engineering materials. Aside from eliminating associated errors to experimental procedures, experimental time and cost were greatly reduced. Computer simulations require no huge cost to material modeling except for cost incurred for getting computer station and application software. This cost is minimal compared to the cost incurred in procuring specimen and setting up experiment rig.

Future work is in the area of considering FE implementation for RF predictive algorithm analysis. This will however require detailed analysis of the hot rolling process to include more than one roll pass. Also, application of RF method together with Monte Carlo simulation to model CCT curves should be considered. This will open up new opportunities for material design software. For constitutive behavior of flexinol wire, a wire-like structure with circular geometry to model the flexinol wire with all boundary conditions is implemented. This will be an added work to the success recorded in this research.

References

- [1] Chen, W., Yin, X., Lee, S., Liu, W.K. “A multiscale design methodology for hierarchical systems with random field uncertainty”. *Journal of Mechanical Design*, vol. 132, no.4, pp. 1-11, 2010.
- [2] Goh, C.H., Ahmed, S., Dachowicz, A.P., Allen, J.K., Mistree, F., “Integrated multiscale robust design considering microstructure evolution and material properties in the hot rolling process”, in *Proceedings of the ASME 2014 International Design Engineering Technical Conferences and Computers and Information in Engineering Conference*, New York, 2014.
- [3] Taguchi, G., “Robust technology development: bringing quality engineering upstream”, *Journal of ASME*, New York, 1993.
- [4] Choi, H. J., McDowell, D.L., Allen, J.K., Rosen, D., Mistree, F., “An inductive design exploration method for robust multiscale materials design”, *The George W. Woodruff School of Mechanical Engineering*, Atlanta, 2011.
- [5] Choi, H. J., Allen, J.K., Rosen, D., McDowell, D. L., Mistree, F., “An inductive design exploration method for the integrated design of multi-scale materials and products”, *Design Engineering technical design automation conference*, Long Beach, CA, 2005.
- [6] Liu, Y., Zhao, T., Ju, W., Shi, S., “Material discovery and design using machine learning”, *The Chinese Ceramic Society, Production and hosting by Elsevier*, Shanghai, China, August 2017.
- [7] Binder, K., Baumgartner, A., *The Monte Carlo method in condensed matter*, Springer, 1995.
- [8] Hohenberg, P., Kohn, W., “Inhomogeneous electron gas”, *Ecole Normale Supérieure: Physical Review*, vol. 136, no. 3B, 1964.
- [9] Kohn, W., Sham, L.J., “Self-consistent equations including exchange and correlation Effects”, *Physical Review*, pp. 140, 1985.
- [10] Alder, B.J., Wainwright, T.E., “Studies in molecular dynamics”, *Journal of Chemical Physics*. vol. 31, no. 2, 1959.
- [11] Rahman, A., “Correlations in the motion of atoms in liquid argon”, *Journal of Chemical Physics*, vol. 136, no. 2A, 1964.
- [12] Chen, L.Q., “Phase-field models for microstructure evolution”, *Annual Review of Condensed Matter*, pp. 32, 2002.

- [13] Steinbach, I., “Phase-field models in materials science”, *Modeling and Simulation in Material Science and Engineering*, pp. 17, 2009.
- [14] Boettinger, W. J., Warren, J. A., Beckermann, C., Karma, A., “Phase-field simulation of solidification”, *Annual Review on Material Research*. vol. 32, pp. 163, 2002.
- [15] Olson, G. B., “Designing a new material world”. Available: www.researchgate.net/publication/235242260 [Accessed May 2000].
- [16] Rajan, K., “Materials informatics”, pp. 8, 2005.
- [17] Hautier, G., Jain, A, Ong, S. P., “From the computer to the laboratory: materials discovery and design using first-principles calculations”. *Journal of Material Science*, pp. 27, 2012.
- [18] Camacho-Zuñiga, C., Ruiz-Treviño, F. A., “A new group contribution scheme to estimate the glass transition temperature for polymers and diluents”. *Industrial Engineering Research*, pp. 42, 2003.
- [19] Yu, X.L., Yi, B., Wang, X.Y., “Prediction of the glass transition temperatures for polymers with artificial neural network”, *Journal of Computational Theory and Chemistry*, pp. 7, 2008.
- [20] Puchala, B., Tarcea, G., Marquis, E.A., Hedstrom, M., Jagadish, H.V., Allison, J.E., “The materials commons: a collaboration platform and information repository for the global materials community”, *Journal of Minerals, Metals, and Materials Society*, vol. 68, no. 8, pp. 2035, 2016.
- [21] Kirklin, S., Saal, J. E., Meredig, B., Thompson, A., Doak, J.W., Aykol, M., “The open quantum materials database (OQMD): assessing the accuracy of DFT formation energies”. *Journal of Computational Material Science*, vol. 1, 2015.
- [22] Belsky, A., Hellenbrandt, M., Karen, V.L., Luksch, P., “New developments in the inorganic crystal structure database (ICSD): accessibility in support of materials research and design”, *Acta Crystallographical Section B Structural Science*, vol. 58, 2002.
- [23] Allen, F.H., “The Cambridge structural database: a quarter of a million crystal structures and rising”. *Acta Crystallographical Section B Structural Science*, vol. 58, 2002.
- [24] Hachmann, J., Olivaresamaya, R., Atahnevrenk, S., Amadorbedolla, C., Sanchezcarrera, S., Goldparker, A., “The Harvard clean energy project; large-scale

- computational screening and design of molecular motifs for organic photovoltaics on the world community grid”, *Journal of Physical Chemistry*, vol. 2, 2011.
- [25] Jain, A., Ong, P., Hautier, G., Chen, W., Richards, D., Dacek, S., “Commentary: the materials project: a materials genome approach to accelerating materials innovation”, *Journal of American Institute of Physics*, vol. 1, no.1, 2013.
- [26] Blaiszik, B., Chard, K., Pruyne, J., Ananthkrishnan, R., Tuecke, S., Foster, I., “The materials data facility: data services to advance materials science research”, *Journal of Minerals, Metals, and Materials Society*, vol. 68, no. 8, pp. 2045, 2016.
- [27] Kusne, A.G., Gao, T., Mehta, A., Ke, L., Nguyen, M.C., Ho, K.-M., “On-the-fly machine-learning for high-throughput experiments: search for rare-earth-free permanent magnets”, *Scientific report Journal*, vol. 4, 2014.
- [28] Murphy, K.P., *Machine learning: a probabilistic perspective*, MA, USA, MIT Press, 2012.
- [29] Mueller T., Kusne A. G., Ramprasad R., “Machine learning in materials science: recent progress and emerging applications”, *Review in Computational Chemistry*, vol. 29, 2016.
- [30] Ghiringhelli, L.M., Vybiral, J., Levchenko, S.V., Draxl, C., Scheffler, M., “Big data of materials science: critical role of the descriptor”, *Physical reviews letter*, vol. 114, no. 10, 2015.
- [31] Arroyave, R., Gibbons, S.L., Galvan, E., Malak, R.J., “The inverse phase stability problem as a constraint satisfaction problem: Application to material design”, *Journal of the Minerals, Metals, and Materials Society*, vol. 68, no. 5, 2016.
- [32] Matthews, J., Klatt, T., Morris, C., Seepersad, C.C., Haberman, M., “Hierarchical design of negative stiffness metamaterials using a Bayesian Network Classifier”, 2014.
- [33] Shai, S.-S., Shai, B.-D., *Understanding machine learning*, USA, Cambridge University Press, 2014.
- [34] Biau, G., “Analysis of a random forest model”, *Journal of Machine learning research*, vol. 13, pp. 1063-1095, 2012.
- [35] Arisoy, Y.M., Özel, T., “Machine learning based predictive modeling of machining induced microhardness and grain size in Ti-6Al-4V alloy”, *Materials and Manufacturing Processes*, vol. 30, no. 4, pp. 425-433, (2015).
- [36] Criminisi, A., Shotton, J., *Decision forests for computer vision and medical image analysis*, Springer, 2013.

- [37] Diaz-Uriarte, R., de Andres, S.A., “Gene selection and classification of microarray data using ‘ random forest”, *BMC Bioinformatics*, vol. 7, pp. 1471–2105, 2006.
- [38] Breiman, L., “Machine learning”, *Journal of Machine Learning Research*, vol. 45, pp. 5–32, 2001.
- [39] Genuer, R., Poggi, J.M., Tuleau-Malot, C., “Random forests: some methodological insights”, *Institut National De Recherche En Informatique Et En Automatique*, 2008.
- [40] Genuer, R., Poggi, J.M., Tuleau-Malot, C., “Variable selection using random forests”, *Pattern Recognition Letters*, vol. 31, pp. 2225–2236, 2010.
- [41] Scornet, E. “Learning with random forests”, Statistics Department, Université Pierre et Marie Curie, 2015.
- [42] Loh, W., “Classification and regression tree methods”. *Encyclopedia of statistics in quality and reliability*, 2008.
- [43] Maalekian, M., “The effects of alloying elements on steels”, *Technische Universitat Graz*, 2007.
- [44] Hougardy, H.P., “Transformation of steels during cooling”, *Theory and Technology of Quenching*. Springer, Berlin, Heidelberg, 1992.
- [45] Pillai, N., Karthikeyan, R., “Prediction of TTT curves of cold working tool steels using support vector machine model”, *IOP Conference Series; Material Science and Engineering*, vol. 346, 2018.
- [46] Ghaboussi, J., Carret, J., Wu, X., “Knowledge-based modeling of material behavior with neural networks”, *Journal of Engineering Mechanics Division*, vol. 17, pp. 32-153, 1991.
- [47] Ghaboussi, J., Sidarta, D.E., “New nested adaptive neural networks (NANN) for constitutive modeling”. *Computers and Geotechnics*, vol. 22, pp. 29-52, 1998.
- [48] Wang, T., Shi, Z., Liu, D., Ma, C., Zhang, Z. “An accurately controlled antagonistic shape memory alloy actuator with self-sensing”, *Sensors*, vol. 12, pp. 7682-7700, 2012.
- [49] Lange, G., Lachmannb, A., Rahim, A., Ismai, M., Low, C., “Shape memory alloys as linear drives in robot hand actuation”, *Procedia Computer Science*, vol. 76, pp. 168 – 173, 2015.

- [50] Ma, N., Song, G., Lee, H., “Position control of shape memory alloy actuators with internal electrical resistance feedback using neural networks”. *Smart Materials and Structures*, vol.13, pp. 777–783, 2004.
- [51] Carballo, M., Pu, Z.J., Wu, K.H., “Variation of electrical resistance and the elastic modulus of shape memory alloys under different loading and temperature conditions”. *Journal of Intelligent Systems and Structures*, vol. 6, pp. 557–565, 1995.
- [52] Gor, F., Carnevale, D., Doro, A.A., Nicosia, S., Pennestri, E., “A new hysteretic behavior in the electrical resistivity of flexinol shape memory alloys versus temperature”, *International Journal of Thermo-physics*, vol. 27, pp. 866-879, 2006.
- [53] Perlis, W.C., Ghazali, M. I. Jamain, S., “Thermo-mechanical properties of shape memory alloy”, Available: www.researchgate.net/publication [Accessed October 2007].

Appendix A

Monte Carlo Algorithm

```
Example Monte Carlo Simulation in Matlab
Function:  $y = -46.13 \cdot \log(x_2) + 483.88$ ;
Generate p samples from a normal distribution
 $r = ( \text{randn}(p,1) * \phi ) + \mu$ 
 $\mu$ : mean
 $\phi$ : standard deviation

Generate p samples from a uniform distribution
 $r = a + \text{rand}(p,1) * (b-a)$ 
a: minimum
b: maximum

p = #value;      The number of function evaluations

--- Generate vectors of random inputs
x1 ~ Normal distribution N
x2 ~ Uniform distribution U

x1 = ( randn(p,1) * 110.70 ) + 360.92;
x2 = 0.772375 + rand(p,1) * ( 203.178 - 0.772375 );

--- Run the simulation
Note the use of element-wise multiplication

y = 445.5*exp(-0.003)*x2;

--- Calculate summary statistics

y_mean = mean(y)
y_std = std(y)
y_median = median(y)

scatter(log(x2),y,2)
```

Appendix B

Random Forest Algorithm

```
## workspace directory getwd()
# clear the workspace for analysis
rm(list=ls())
# Import dataset into r environment
# Initiate the Random Forest Algorithm from the library
library(readxl)
library(randomForest)
P<- read_excel("A8steelcct.xlsx", sheet="Sheet2")
##Setting the seed so that results will be the same each time I run Random Forest
set.seed(1234)
DataFrame<-P
str(DataFrame)
df<- DataFrame
dim(DataFrame)
head(DataFrame,3)
summary(df)
mean(df$p)
max(df$p)
###To create the train and test data set
####target variable is UTS (ultimate tensile strength)
fractionTraining <- 0.9
fractionTest <- 0.1
#compute sample sizes
sampleSizeTraining <- floor(fractionTraining * nrow(df))
sampleSizeTest <- floor(fractionTest * nrow(df))
#create the randomly-sampled indices for the dataframe to avoid overlapping subsets of indices
indicesTraining <- sort(sample(seq_len(nrow(df)), size = sampleSizeTraining))
indicesNotTraining <- setdiff(seq_len(nrow(df)), indicesTraining)
indicesTest <- sort(sample(seq_len(nrow(df)), size = sampleSizeTest))
```



```

#Finally, output the two dataframes for training and test
dfTraining <- df[indicesTraining, ]
dfTest <- df[indicesTest, ]
View(dfTest)
View(dfTraining)
#fitting the model
modelRandom<-randomForest(p~.,data = dfTraining,mtry=3,ntree=800)
modelRandom
PredictiveRegression<- predict(modelRandom, dfTest, type = 'response')
t<-table(predictions=PredictiveRegression, actual=dfTest$p)
t
print(t)
#calculating MSE
model= lm(p~.,data = df)
mse_test<-mean((df$p - predict.lm(model,df))^2)
summary(model)
#accuracy metric
sum(diag(t))/sum(t)
write.table(t, file = "Nike.csv", sep=",")

```

Appendix C

ANSYS Report File



Project

First Saved	Tuesday, March 27, 2018
Last Saved	Friday, April 5, 2019
Product Version	19.2 Release
Save Project Before Solution	No
Save Project After Solution	No

TABLE 1

Unit System	Metric (mm, kg, N, s, mV, mA) Degrees rad/s Celsius
Angle	Degrees
Rotational Velocity	rad/s
Temperature	Celsius

Model (A4)

Geometry

TABLE 2
Model (A4) > Geometry

Object Name	<i>Geometry</i>
State	Fully Defined
Definition	
Source	E:\ansysdata\studentcommunity\Material Model Test Block\Material Model Test Block 2_files\dp0\SYSDM\SYS.agdb
Type	DesignModeler
Length Unit	Meters
Element Control	Program Controlled
Display Style	Body Color
Bounding Box	
Length X	1. mm
Length Y	1. mm
Length Z	1. mm
Properties	
Volume	1. mm ³
Mass	7.85e-006 kg

Scale Factor Value	1.
Statistics	
Bodies	1
Active Bodies	1
Nodes	20
Elements	1
Mesh Metric	None
Update Options	
Assign Default Material	No
Basic Geometry Options	
Parameters	Independent
Parameter Key	
Attributes	Yes
Attribute Key	
Named Selections	Yes
Named Selection Key	
Material Properties	Yes
Advanced Geometry Options	
Use Associativity	Yes
Coordinate Systems	Yes
Coordinate System Key	
Reader Mode Saves Updated File	No
Use Instances	Yes
Smart CAD Update	Yes
Compare Parts On Update	No
Analysis Type	3-D
Clean Bodies On Import	No
Stitch Surfaces On Import	No
Decompose Disjoint Geometry	Yes
Enclosure and Symmetry Processing	Yes

TABLE 3
Model (A4) > Geometry > Parts

Object Name	<i>Solid</i>
State	Meshed
Graphics Properties	
Visible	Yes

Transparency	1
Definition	
Suppressed	No
Stiffness Behavior	Flexible
Coordinate System	Default Coordinate System
Reference Temperature	By Environment
Behavior	None
Material	
Assignment	EPP 250 MPa
Nonlinear Effects	Yes
Thermal Strain Effects	Yes
Bounding Box	
Length X	1. mm
Length Y	1. mm
Length Z	1. mm
Properties	
Volume	1. mm ³
Mass	7.85e-006 kg
Centroid X	0.5 mm
Centroid Y	0.5 mm
Centroid Z	0.5 mm
Moment of Inertia Ip1	1.3083e-006 kg·mm ²
Moment of Inertia Ip2	1.3083e-006 kg·mm ²
Moment of Inertia Ip3	1.3083e-006 kg·mm ²
Statistics	
Nodes	20
Elements	1
Mesh Metric	None

Coordinate Systems

TABLE 4
Model (A4) > Coordinate Systems > Coordinate System

Object Name	<i>Global Coordinate System</i>	<i>XYPlane</i>	<i>ZXPlane</i>
State	Fully Defined		
Definition			
Type	Cartesian		
Coordinate System ID	0.		
Coordinate System		Program Controlled	
APDL Name			
Suppressed		No	
Origin			
Origin X	0. mm		
Origin Y	0. mm		
Origin Z	0. mm		

Define By		Global Coordinates
Location		Defined
Directional Vectors		
X Axis Data	[1. 0. 0.]	[0. 0. 1.]
Y Axis Data	[0. 1. 0.]	[1. 0. 0.]
Z Axis Data	[0. 0. 1.]	[0. 1. 0.]
Principal Axis		
Axis		X
Define By		Fixed Vector
Orientation About Principal Axis		
Axis		Y
Define By		Fixed Vector
Transformations		
Base Configuration		Absolute
Transformed Configuration		[0. 0. 0.]

Symmetry

TABLE 5
Model (A4) > Symmetry

Object Name	<i>Symmetry</i>
State	Fully Defined

TABLE 6
Model (A4) > Symmetry > Symmetry Region

Object Name	<i>Symmetry Region</i>	<i>Symmetry Region 2</i>	<i>Symmetry Region 3</i>
State	Fully Defined		
Scope			
Scoping Method	Named Selection		Geometry Selection
Named Selection	Symmetry:XYPlane	Symmetry:ZXPlane	
Geometry			1 Face
Definition			
Scope Mode	Automatic		Manual
Type	Symmetric		
Coordinate System	XYPlane	ZXPlane	Global Coordinate System
Symmetry Normal	Z Axis		X Axis
Suppressed	No		

Mesh

TABLE 7
Model (A4) > Mesh

Object Name	<i>Mesh</i>
State	Solved
Display	

Display Style	Use Geometry Setting
Defaults	
Physics Preference	Mechanical
Element Order	Program Controlled
Element Size	2.0 mm
Sizing	
Use Adaptive Sizing	No
Growth Rate	Default (1.85)
Max Size	Default (4.0 mm)
Mesh Defeaturing	Yes
Defeature Size	Default (1.e-002 mm)
Capture Curvature	No
Capture Proximity	No
Bounding Box Diagonal	1.7321 mm
Average Surface Area	1.0 mm ²
Minimum Edge Length	1.0 mm
Quality	
Check Mesh Quality	Yes, Errors
Error Limits	Standard Mechanical
Target Quality	Default (0.050000)
Smoothing	Medium
Mesh Metric	None
Inflation	
Use Automatic Inflation	None
Inflation Option	Smooth Transition
Transition Ratio	0.272
Maximum Layers	5
Growth Rate	1.2
Inflation Algorithm	Pre
View Advanced Options	No
Advanced	
Number of CPUs for Parallel Part Meshing	Program Controlled
Straight Sided Elements	No
Rigid Body Behavior	Dimensionally Reduced
Triangle Surface Mesher	Program Controlled
Topology Checking	No
Pinch Tolerance	Default (1.8e-002 mm)
Generate Pinch on Refresh	No
Statistics	
Nodes	20
Elements	1

Named Selections

TABLE 8
Model (A4) > Named Selections > Named Selections

Object Name	<i>Symmetry:XYPlane</i> <i>Symmetry:ZXPlane</i>
State	Fully Defined
Scope	
Scoping Method	Geometry Selection
Geometry	1 Face
Definition	
Send to Solver	No
Protected	Program Controlled
Visible	Yes
Program Controlled Inflation	Exclude
Statistics	
Type	Imported
Total Selection	1 Face
Surface Area	1. mm ²
Suppressed	0
Used by Mesh Worksheet	No

Static Structural (A5)

TABLE 9
Model (A4) > Analysis

Object Name	<i>Static Structural (A5)</i>
State	Solved
Definition	
Physics Type	Structural
Analysis Type	Static Structural
Solver Target	Mechanical APDL
Options	
Environment Temperature	22. °C
Generate Input Only	No

TABLE 10
Model (A4) > Static Structural (A5) > Analysis Settings

Object Name	<i>Analysis Settings</i>
State	Fully Defined
Step Controls	
Number Of Steps	2.
Current Step Number	2.
Step End Time	2. s
Auto Time Stepping	On

Define By	Substeps
Carry Over Time Step	Off
Initial Substeps	20.
Minimum Substeps	20.
Maximum Substeps	20.
Solver Controls	
Solver Type	Program Controlled
Weak Springs	Off
Solver Pivot Checking	Program Controlled
Large Deflection	Off
Inertia Relief	Off
Rotordynamics Controls	
Coriolis Effect	Off
Restart Controls	
Generate Restart Points	Program Controlled
Retain Files After Full Solve	No
Combine Restart Files	Program Controlled
Nonlinear Controls	
Newton-Raphson Option	Program Controlled
Force Convergence	Program Controlled
Moment Convergence	Program Controlled
Displacement Convergence	Program Controlled
Rotation Convergence	Program Controlled
Line Search	Program Controlled
Stabilization	Off
Output Controls	
Stress	Yes
Strain	Yes
Nodal Forces	No
Contact Miscellaneous	No
General Miscellaneous	No
Store Results At	All Time Points
Analysis Data Management	

Solver Files Directory	C:\Users\joll\l\AppData\Local\Temp\Material Model Test Block Bilinear Kinematic Hardening.tmp\Material Model Test Block Bilinear Kinematic Hardening_files\dp0\SYSMECH\
Future Analysis	None
Scratch Solver Files Directory	
Save MAPDL db	No
Contact Summary	Program Controlled
Delete Unneeded Files	Yes
Nonlinear Solution	Yes
Solver Units	Active System
Solver Unit System	nmm

TABLE 11
Model (A4) > Static Structural (A5) > Analysis Settings
Step-Specific "Step Controls"

Step	Step End Time	Maximum Substeps	Carry Over Time Step
1	1. s	100.	
2	2. s	20.	Off

TABLE 12
Model (A4) > Static Structural (A5) > Loads

Object Name	<i>Displacement</i>
State	Fully Defined
Scope	
Scoping Method	Geometry Selection
Geometry	1 Face
Definition	
Type	Displacement
Define By	Components
Coordinate System	Global Coordinate System
X Component	Free
Y Component	Tabular Data
Z Component	Free
Suppressed	No
Tabular Data	
Independent Variable	Time

FIGURE 1
Model (A4) > Static Structural (A5) > Displacement

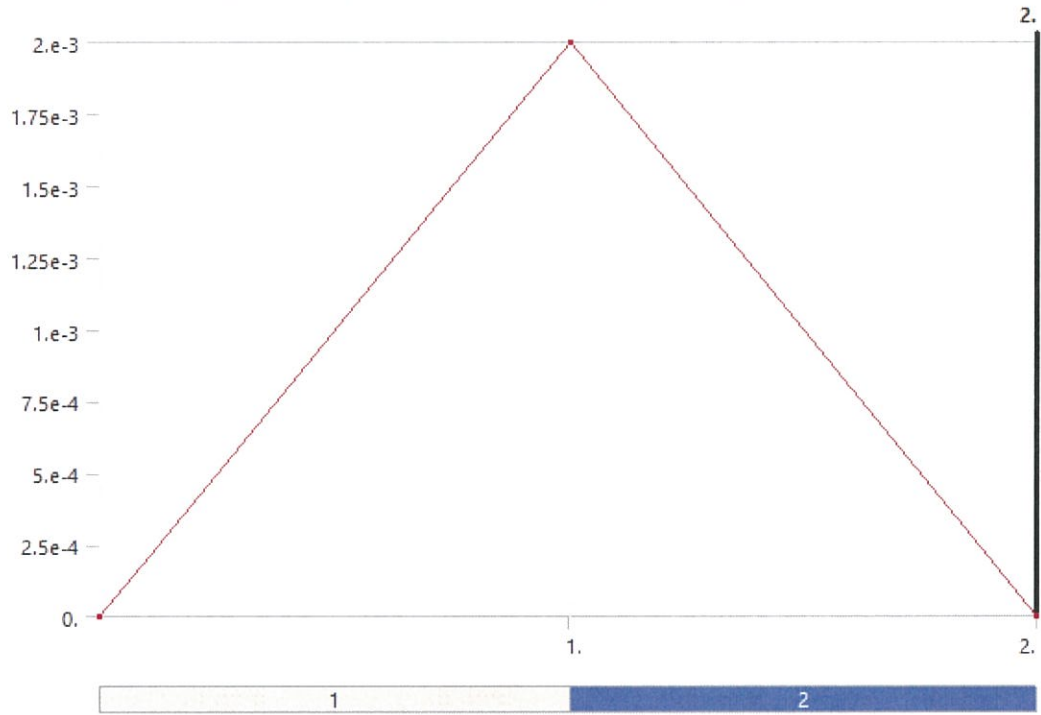


TABLE 13
Model (A4) > Static Structural (A5) > Displacement

Steps	Time [s]	Y [mm]
1	0.	0.
	1.	2.e-003
2	2.	0.

Solution (A6)

TABLE 14
Model (A4) > Static Structural (A5) > Solution

Object Name	<i>Solution (A6)</i>
State	Solved
Adaptive Mesh Refinement	
Max Refinement Loops	1.
Refinement Depth	2.
Information	
Status	Done
MAPDL Elapsed Time	3. s
MAPDL Memory Used	22. MB

MAPDL Result File Size	576. KB
Post Processing	
Beam Section Results	No
On Demand Stress/Strain	No

TABLE 15
Model (A4) > Static Structural (A5) > Solution (A6) > Solution Information

Object Name	<i>Solution Information</i>
State	Solved
Solution Information	
Solution Output	Solver Output
Newton-Raphson Residuals	0
Identify Element Violations	0
Update Interval	2.5 s
Display Points	All
FE Connection Visibility	
Activate Visibility	Yes
Display	All FE Connectors
Draw Connections Attached To	All Nodes
Line Color	Connection Type
Visible on Results	No
Line Thickness	Single
Display Type	Lines

TABLE 16
Model (A4) > Static Structural (A5) > Solution (A6) > Results

Object Name	<i>Equivalent Total Strain</i>	<i>Equivalent Stress</i>
State	Solved	
Scope		
Scoping Method	Geometry Selection	
Geometry	All Bodies	
Definition		
Type	Equivalent Total Strain	Equivalent (von-Mises) Stress
By	Time	
Display Time	Last	1. s
Calculate Time History	Yes	
Identifier		
Suppressed	No	
Integration Point Results		
Display Option	Averaged	
Average Across Bodies	No	
Results		
Minimum	1.5e-003 mm/mm	250. MPa

Maximum	1.5e-003 mm/mm	250. MPa
Average	1.5e-003 mm/mm	250. MPa
Minimum Occurs On	Solid	
Maximum Occurs On	Solid	
Minimum Value Over Time		
Minimum	1.e-004 mm/mm	10. MPa
Maximum	2.e-003 mm/mm	250. MPa
Maximum Value Over Time		
Minimum	1.e-004 mm/mm	10. MPa
Maximum	2.e-003 mm/mm	250. MPa
Information		
Time	2. s	1. s
Load Step	2	1
Substep	20	
Iteration Number	44	23

FIGURE 2
Model (A4) > Static Structural (A5) > Solution (A6) > Equivalent Total Strain

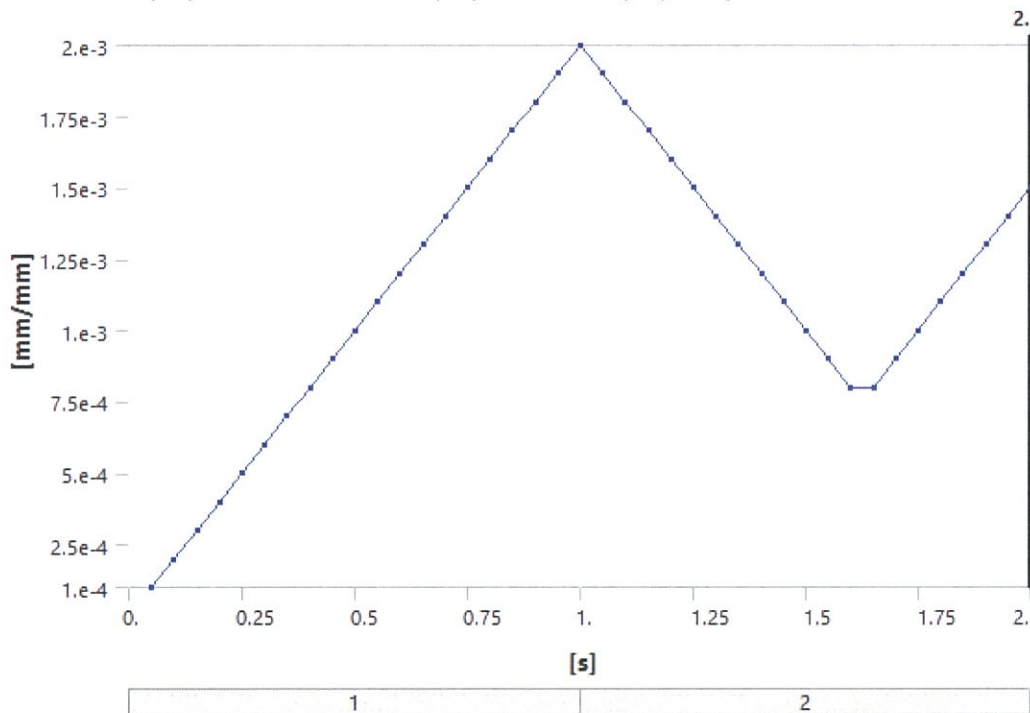


TABLE 17
Model (A4) > Static Structural (A5) > Solution (A6) > Equivalent Total Strain

Time [s]	Minimum [mm/mm]	Maximum [mm/mm]	Average [mm/mm]
----------	-----------------	-----------------	-----------------

5.e-002	1.e-004	1.e-004	1.e-004
0.1	2.e-004	2.e-004	2.e-004
0.15	3.e-004	3.e-004	3.e-004
0.2	4.e-004	4.e-004	4.e-004
0.25	5.e-004	5.e-004	5.e-004
0.3	6.e-004	6.e-004	6.e-004
0.35	7.e-004	7.e-004	7.e-004
0.4	8.e-004	8.e-004	8.e-004
0.45	9.e-004	9.e-004	9.e-004
0.5	1.e-003	1.e-003	1.e-003
0.55	1.1e-003	1.1e-003	1.1e-003
0.6	1.2e-003	1.2e-003	1.2e-003
0.65	1.3e-003	1.3e-003	1.3e-003
0.7	1.4e-003	1.4e-003	1.4e-003
0.75	1.5e-003	1.5e-003	1.5e-003
0.8	1.6e-003	1.6e-003	1.6e-003
0.85	1.7e-003	1.7e-003	1.7e-003
0.9	1.8e-003	1.8e-003	1.8e-003
0.95	1.9e-003	1.9e-003	1.9e-003
1.	2.e-003	2.e-003	2.e-003
1.05	1.9e-003	1.9e-003	1.9e-003
1.1	1.8e-003	1.8e-003	1.8e-003
1.15	1.7e-003	1.7e-003	1.7e-003
1.2	1.6e-003	1.6e-003	1.6e-003
1.25	1.5e-003	1.5e-003	1.5e-003
1.3	1.4e-003	1.4e-003	1.4e-003
1.35	1.3e-003	1.3e-003	1.3e-003
1.4	1.2e-003	1.2e-003	1.2e-003
1.45	1.1e-003	1.1e-003	1.1e-003
1.5	1.e-003	1.e-003	1.e-003
1.55	9.e-004	9.e-004	9.e-004
1.6	8.e-004	8.e-004	8.e-004
1.65			
1.7	9.e-004	9.e-004	9.e-004
1.75	1.e-003	1.e-003	1.e-003
1.8	1.1e-003	1.1e-003	1.1e-003
1.85	1.2e-003	1.2e-003	1.2e-003
1.9	1.3e-003	1.3e-003	1.3e-003
1.95	1.4e-003	1.4e-003	1.4e-003
2.	1.5e-003	1.5e-003	1.5e-003

FIGURE 3
Model (A4) > Static Structural (A5) > Solution (A6) > Equivalent Stress

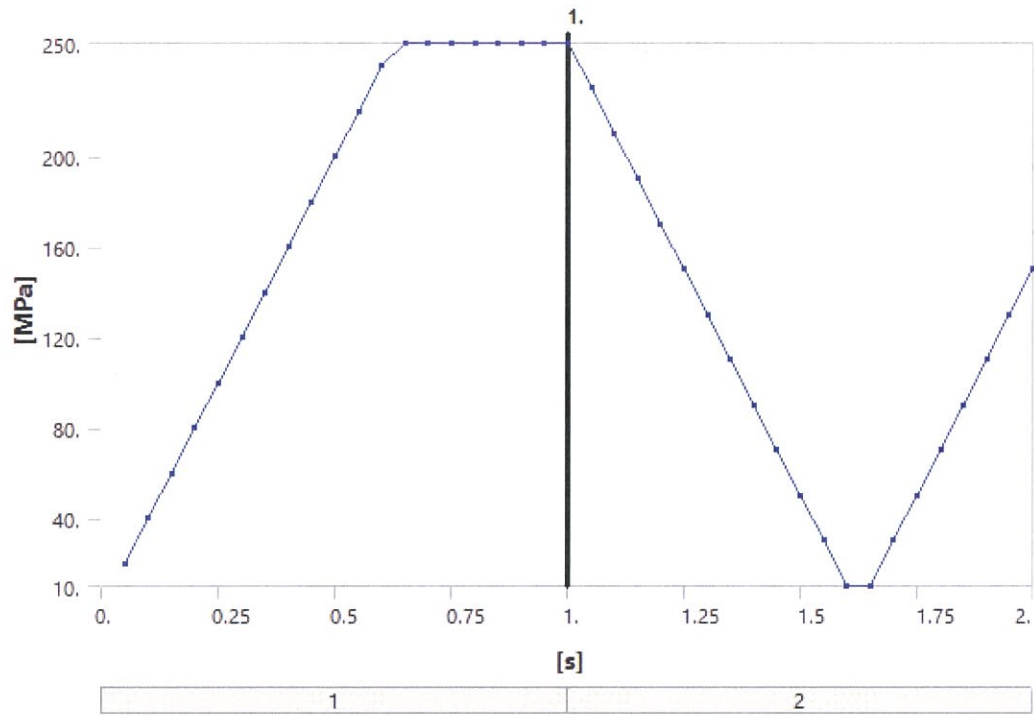


TABLE 18
Model (A4) > Static Structural (A5) > Solution (A6) > Equivalent Stress

Time [s]	Minimum [MPa]	Maximum [MPa]	Average [MPa]
5.e-002	20.	20.	20.
0.1	40.	40.	40.
0.15	60.	60.	60.
0.2	80.	80.	80.
0.25	100.	100.	100.
0.3	120.	120.	120.
0.35	140.	140.	140.
0.4	160.	160.	160.
0.45	180.	180.	180.
0.5	200.	200.	200.
0.55	220.	220.	220.
0.6	240.	240.	240.
0.65	250.	250.	250.
0.7			
0.75			
0.8			
0.85			
0.9			
0.95			
1.			

1.05	230.	230.	230.
1.1	210.	210.	210.
1.15	190.	190.	190.
1.2	170.	170.	170.
1.25	150.	150.	150.
1.3	130.	130.	130.
1.35	110.	110.	110.
1.4	90.	90.	90.
1.45	70.	70.	70.
1.5	50.	50.	50.
1.55	30.	30.	30.
1.6	10.	10.	10.
1.65			
1.7	30.	30.	30.
1.75	50.	50.	50.
1.8	70.	70.	70.
1.85	90.	90.	90.
1.9	110.	110.	110.
1.95	130.	130.	130.
2.	150.	150.	150.

Material Data TABLE 20

Density	7.85e-006 kg mm ⁻³
Isotropic Secant Coefficient of Thermal Expansion	1.2e-005 C ⁻¹
Specific Heat Constant Pressure	4.34e+005 mJ kg ⁻¹ C ⁻¹
Isotropic Thermal Conductivity	6.05e-002 W mm ⁻¹ C ⁻¹
Isotropic Resistivity	1.7e-004 ohm mm

TABLE 19
Steel EPP 250 MPa > S-N Curve

Alternating Stress MPa	Cycles	Mean Stress MPa
3999	10	0
2827	20	0
1896	50	0
1413	100	0
1069	200	0
441	2000	0
262	10000	0
214	20000	0
138	1.e+005	0
114	2.e+005	0
86.2	1.e+006	0